Selective Examples of Molecular Glue: Target Protein Degradation

Baicheng Chen

College of Chemistry and Molecular Engineering

May. 11th, 2024

Contents

The concept of molecular glues

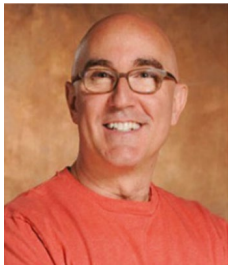

- Molecular glues induce a novel interaction between two proteins and form a ternary complex, leading to diverse biological and pharmacological functions.

calcineurin B **calcineurin A**

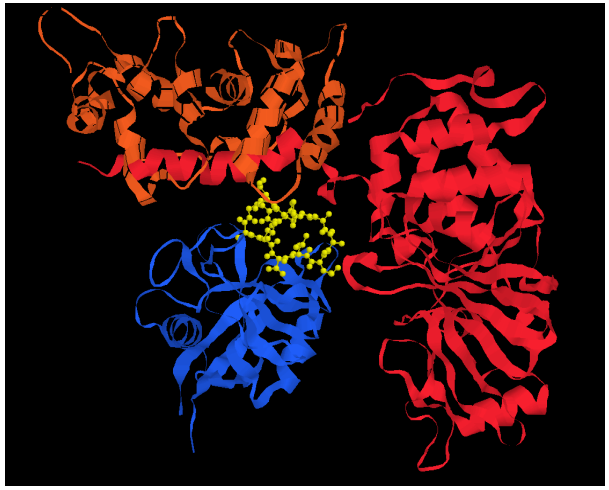

cyclophilin

cyclophilin-CsA-calcineurin
Liu, J. *et al. Cell* **1991**, *66*, 807

calcineurin B **calcineurin A**

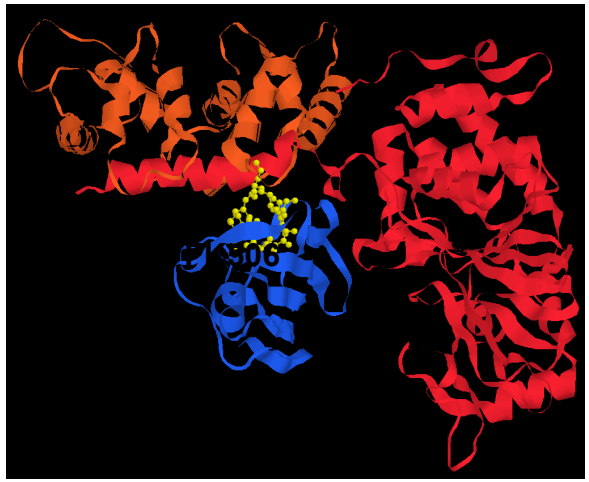

FKBP12

FKBP12-FK506-calcineurin
Liu, J. *et al. Cell* **1991**, *66*, 807

FRB **FKBP12**

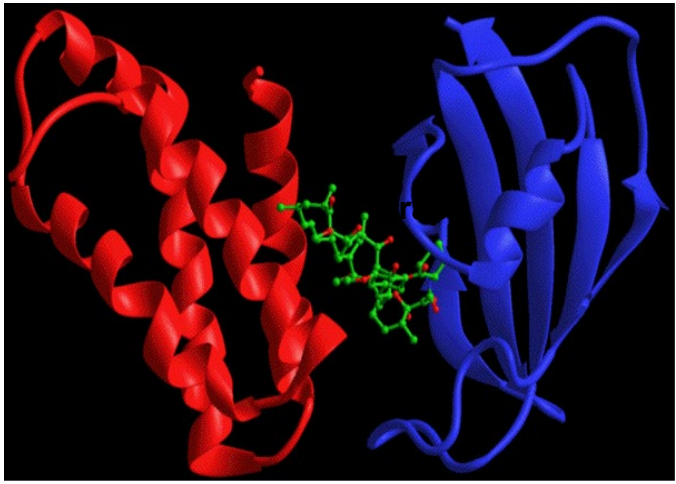

Rapamycin

FKBP12-rapamycin-mTOR
Brown, E. *et al. Nature* **1994** *369*, 756
Sabatini, D. *et al. Cell* **1994**, *78*, 35

"Immunophilin-Sensitive Phosphatase Action in Signaling" Schreiber, S. L. *Cell* **1992**, *70*, 365.
"Small Molecule Dimerizers" Crabtree, G. R.; Schreiber, S. L. *TIBS* **1996**, *21*, 418.

Structure of the ternary complex

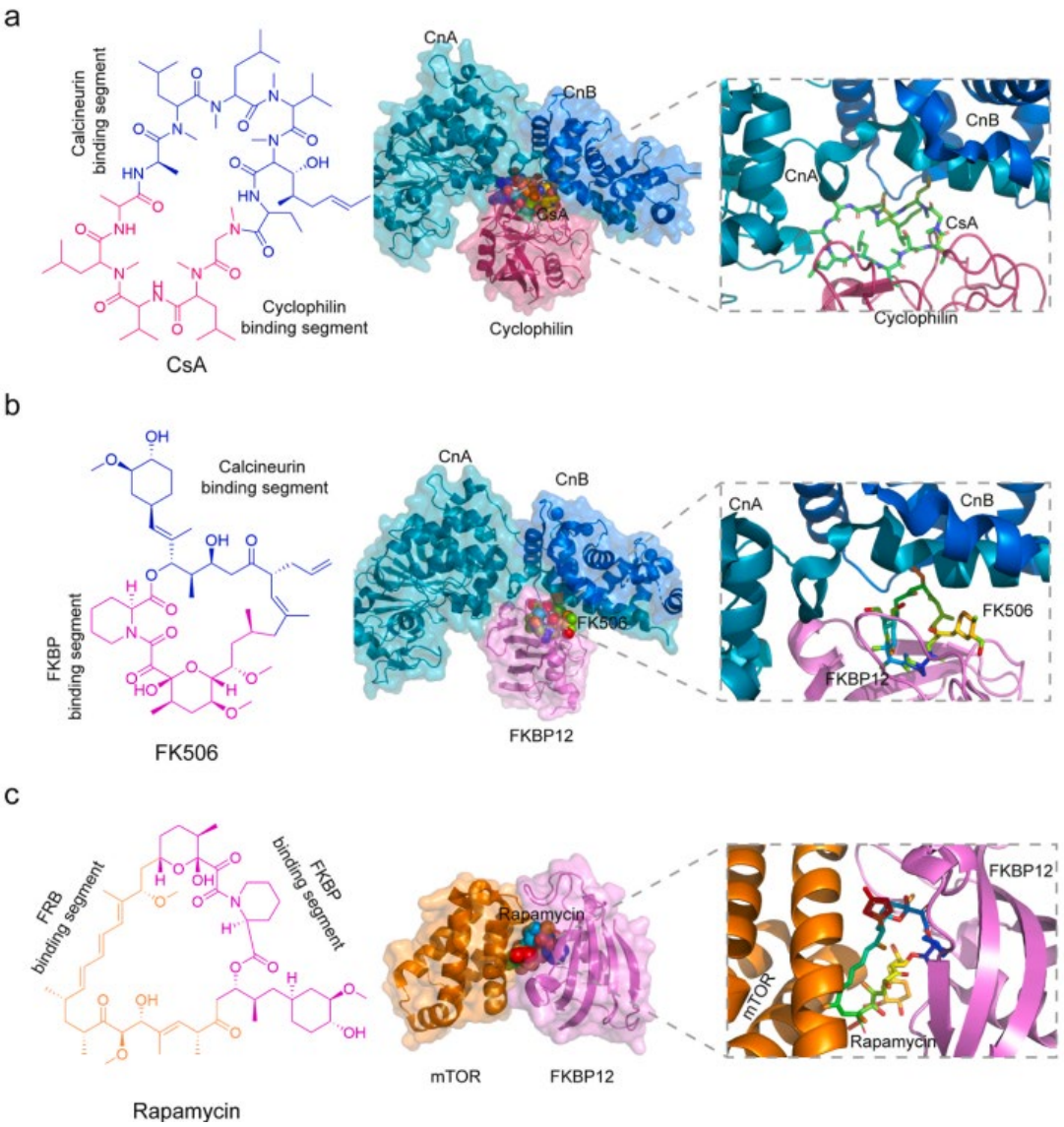

History of molecular glues (MGs)

12 years after cyclosporin's first success in controlling transplant rejection, and 8 years after it is approved by the FDA, its mechanism as a molecular glue is revealed, and the term "molecular glue" is coined.

First mouse study using a designed molecular glue with a linker to target destruction of a specific cell type *in vivo*.

Rapamycin is FDA-approved as an immunosuppressive drug (sirolimus) for transplantation

1991

1993

1996

2000

The first discoveries of molecular glues

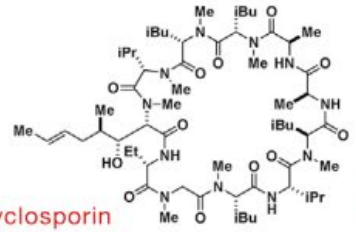

Cyclosporin

Cyclophilin

Calcineurin A
Calcineurin B

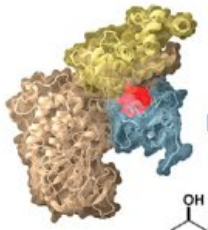

FKBP12

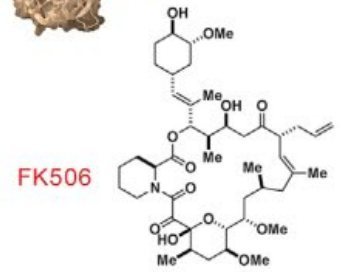

FK506

The first designed molecular glue (CIP/CID)

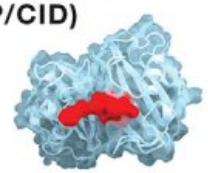

FKBP12

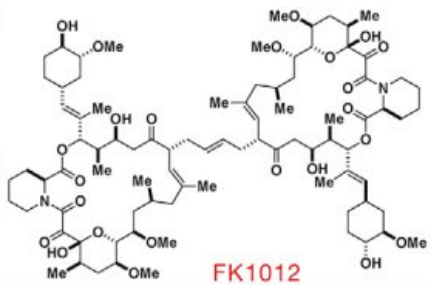

FK1012

The first designed heterodimerizer (CIP/CID)

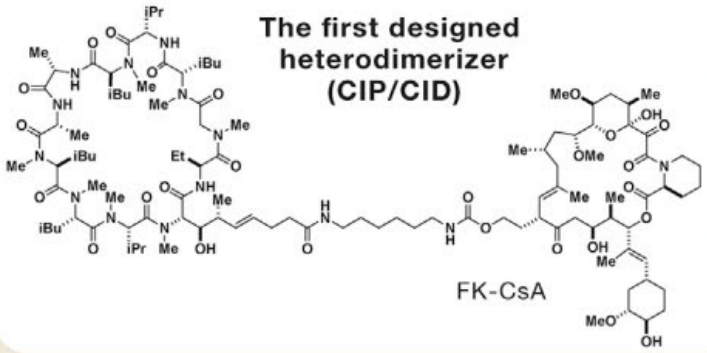

FK-CsA

The first structural analysis of a molecular glue complex

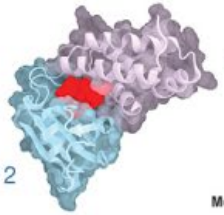

FRB domain of mTOR

FKBP12

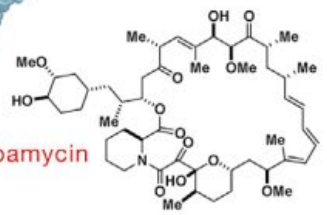

Rapamycin

First application of molecular glue

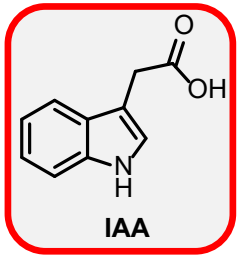

- Auxin enhances the TIR1–substrate interactions mainly by filling in a hydrophobic cavity at the protein interface, leading to its ubiquitin-ligase-catalysed degradation to regulate gene expression

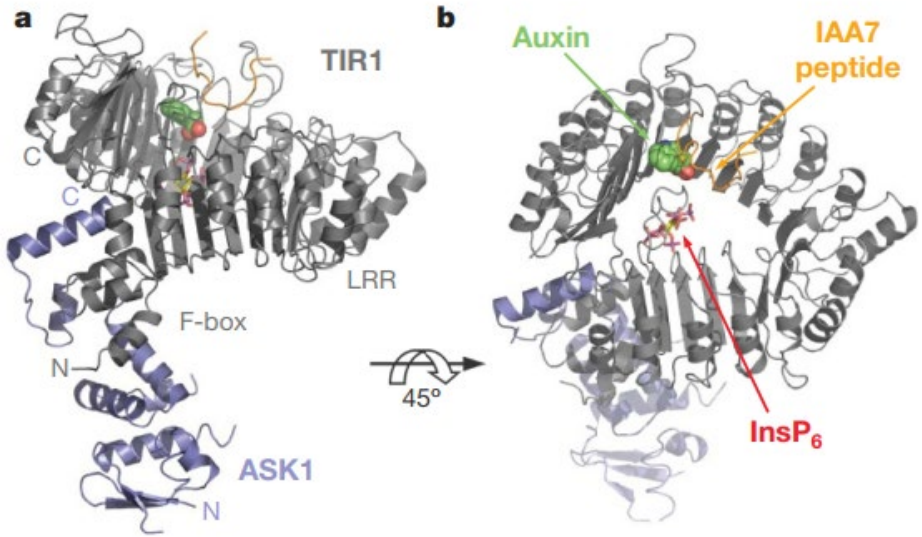

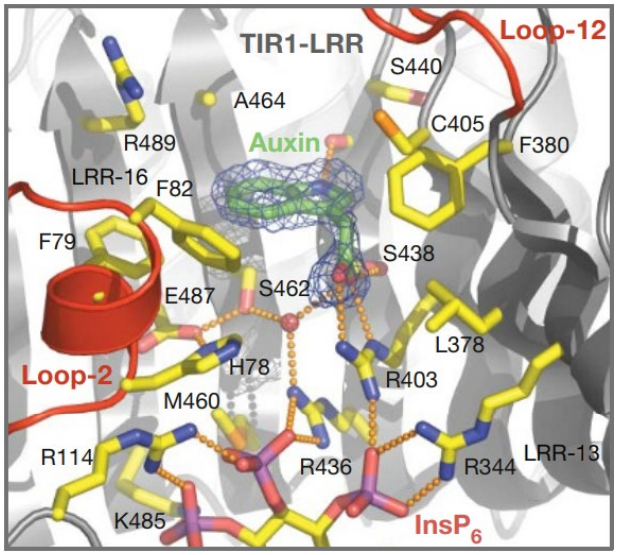

Tan, X., Calderon-Villalobos, L., Sharon, M. et al. *Nature,* **2007**, *446*, 640.

Contents

Renaissance of thalidomide

Gilla Kaplan

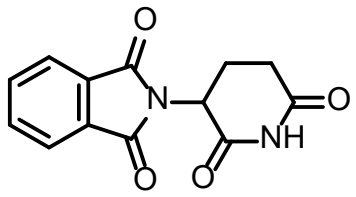

Thalidomide

- Thalidomide selectively inhibits the production of human monocyte tumor necrosis factor α (TNF- α)

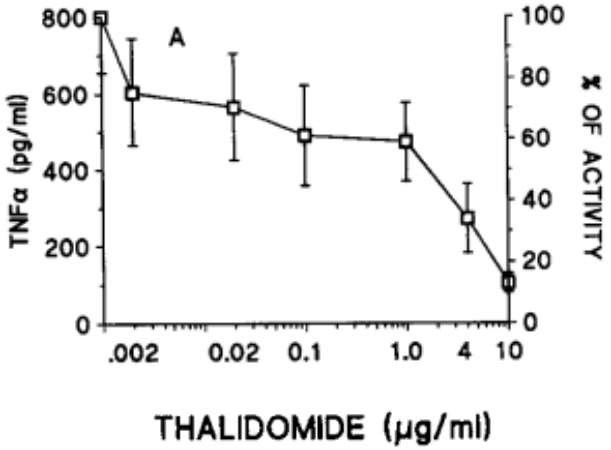

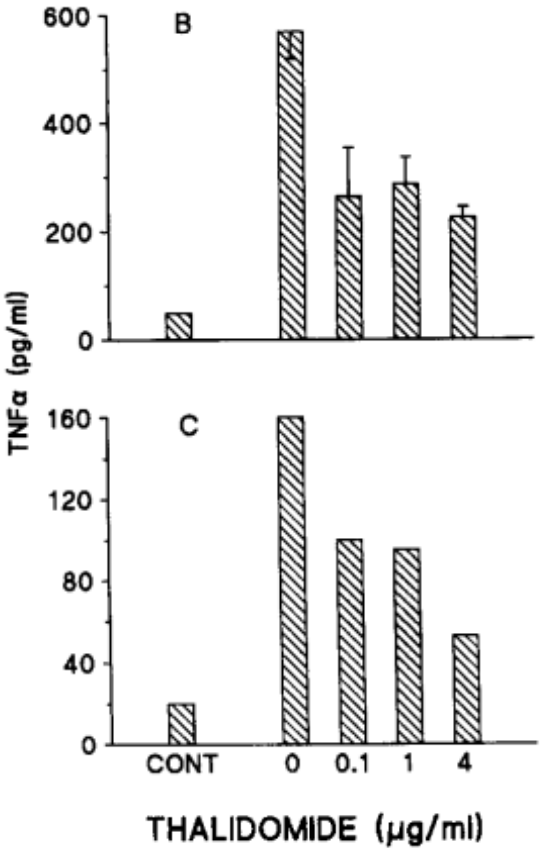

Sampaio, E. P., Sarno, E. N., Galilly, R., Cohn, Z. A., Kaplan, G. *J. Exp. Med.* **1991**, *173*, 699.

Thalidomide bond to CRBN

Celgene (now BMS)

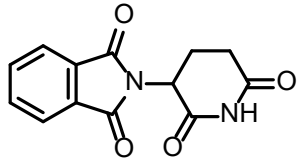

Thalidomide

Approved by FDA in 1998 for severe erythema nodosum leprosum (ENL)

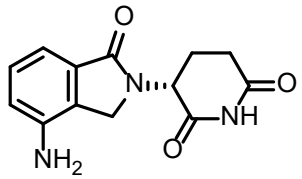

Lenalidomide

Approved by FDA in 2005 for multiple myeloma(MM)

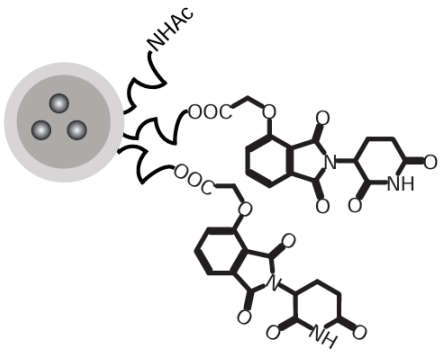

Thal-immobilized beads

Kd=8.5nm

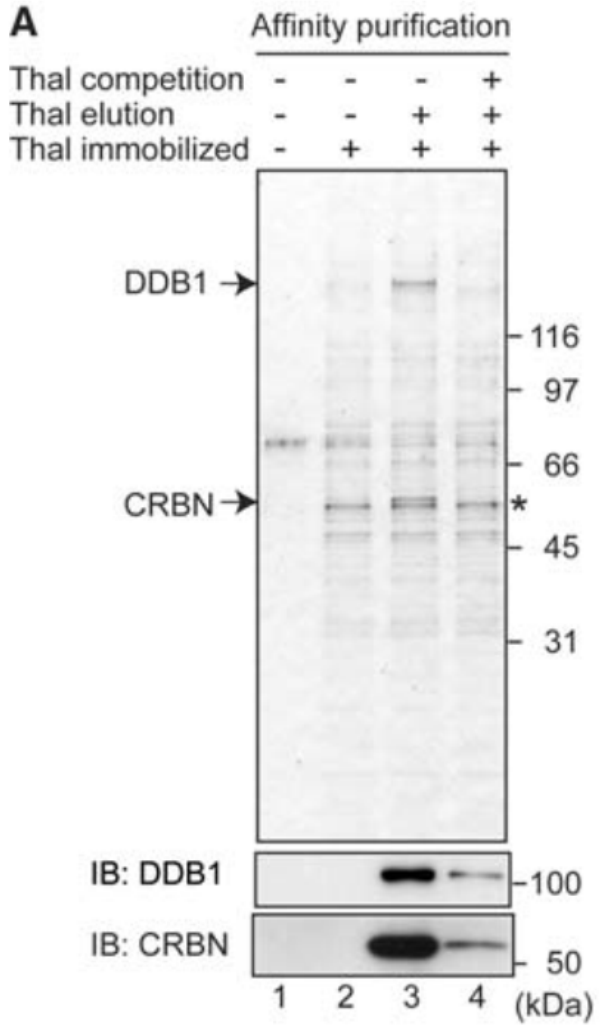

Ito, T. et al. *Science,* **2010**, *327*, 1345.

Mechanism of ubiquitination

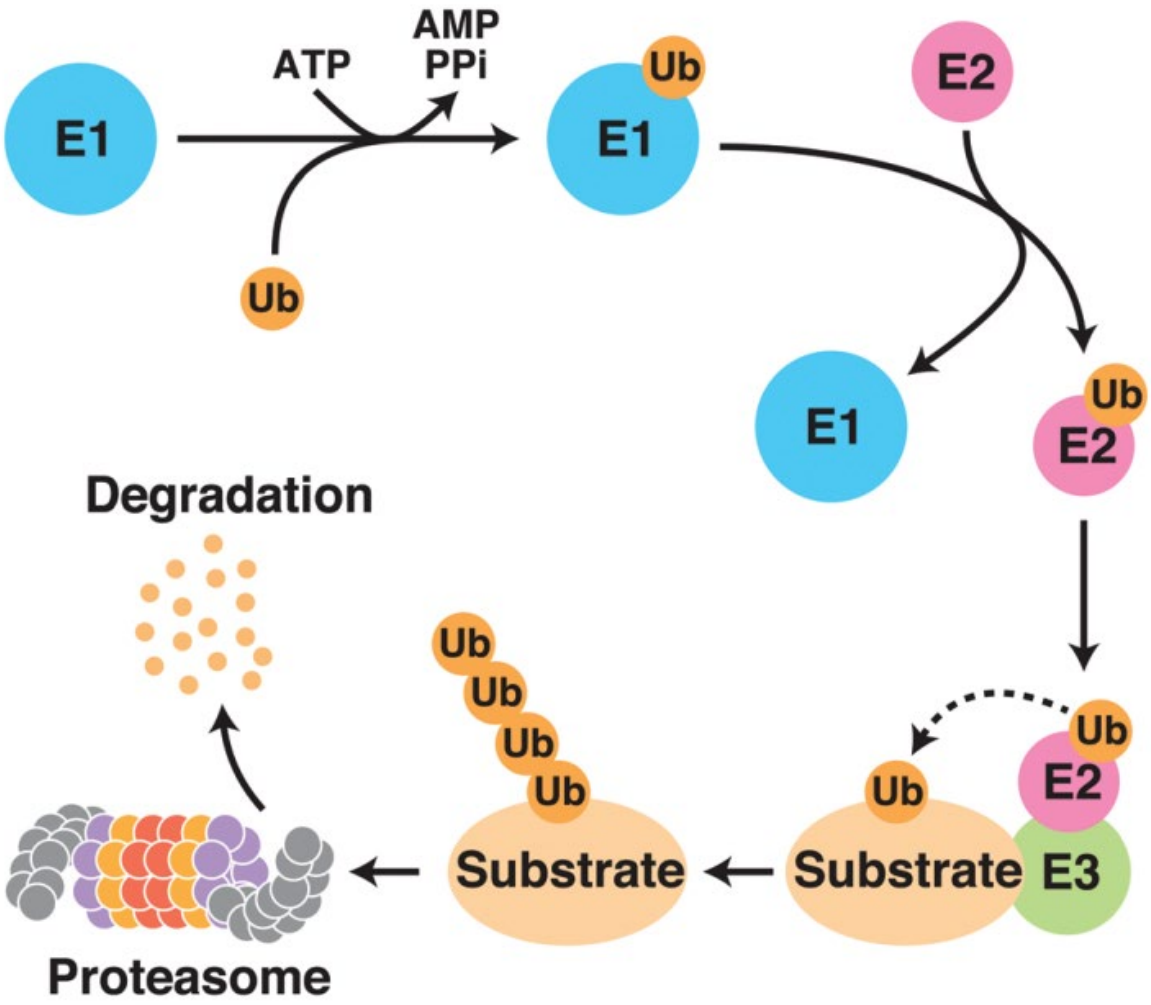

Yamamoto, J., Ito, T., Yamaguchia, Y., Handa, H. *Chem. Soc. Rev.* **2022**, *51*, 6234.

Thalidomide causes degradation of IKZF1 and IKZF3

- Ubiquitin-modified proteome analysis by enriching peptides containing ubiquitinated lysine residues
- Stable isotope labeling of amino acids (SILAC)-based quantitative MS

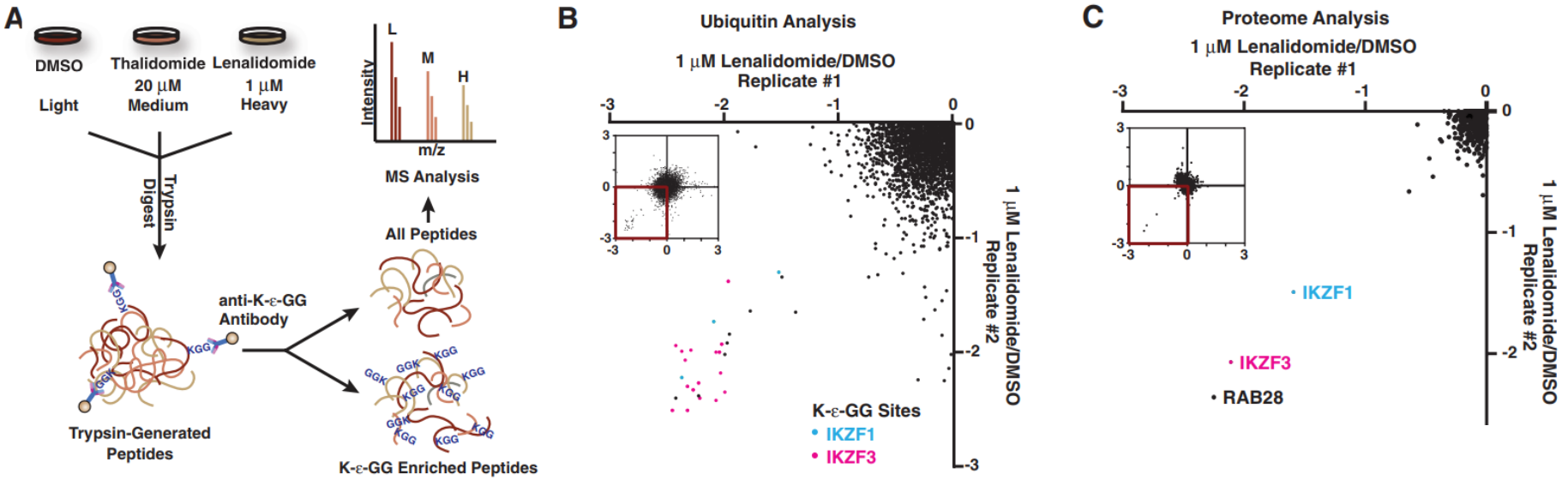

Krönke, J. et al. *Science,* **2014**, *343*, 301.

Crystal structure of thalidomide and CRBN

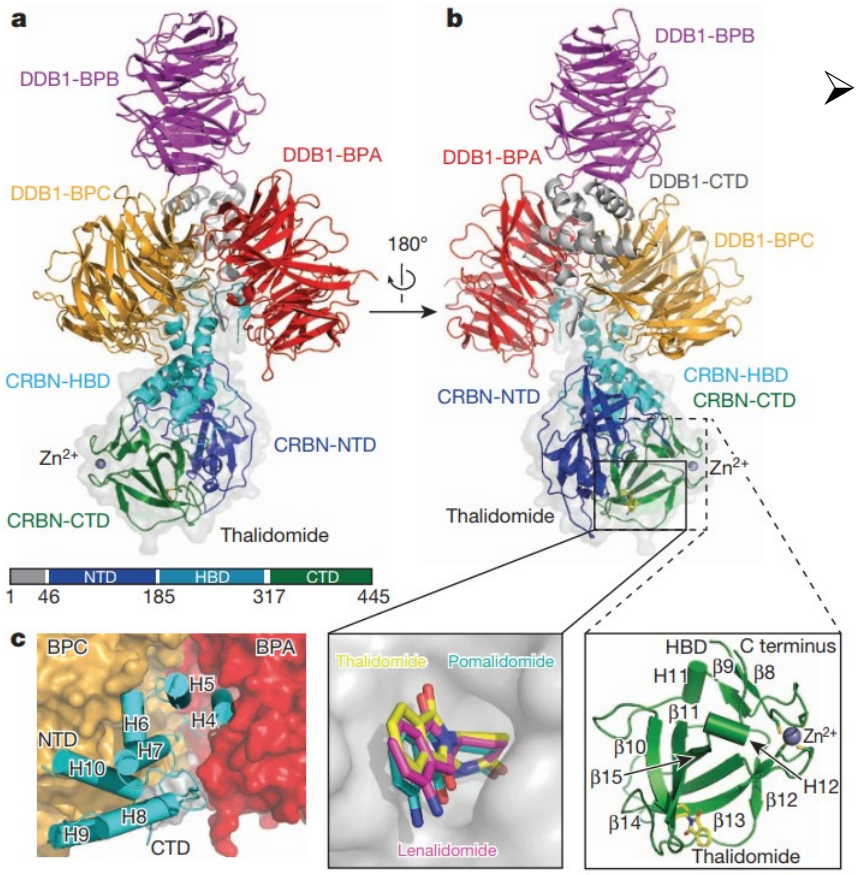

- His380, Trp382, Trp388 in the TBD are required for thalidomide binding
- The isoindolinone ring protrudes outward and is exposed on the surface of CRBN

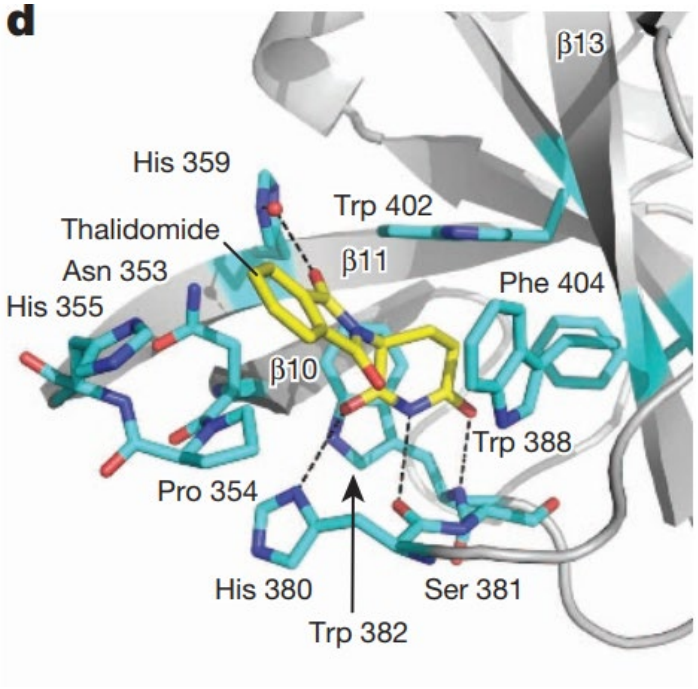

Fischer, E., Böhm, K., Lydeard, J. et al. *Nature,* **2014,** *512*, 49.

Crystal structure of the ternary complex

- CK1α is a multifunctional serine/threonine kinase
- The phthalimide ring of lenalidomide is surface exposed. A β-hairpin loop of CK1α binds CRBN on top of its lenalidomide-binding pocket.

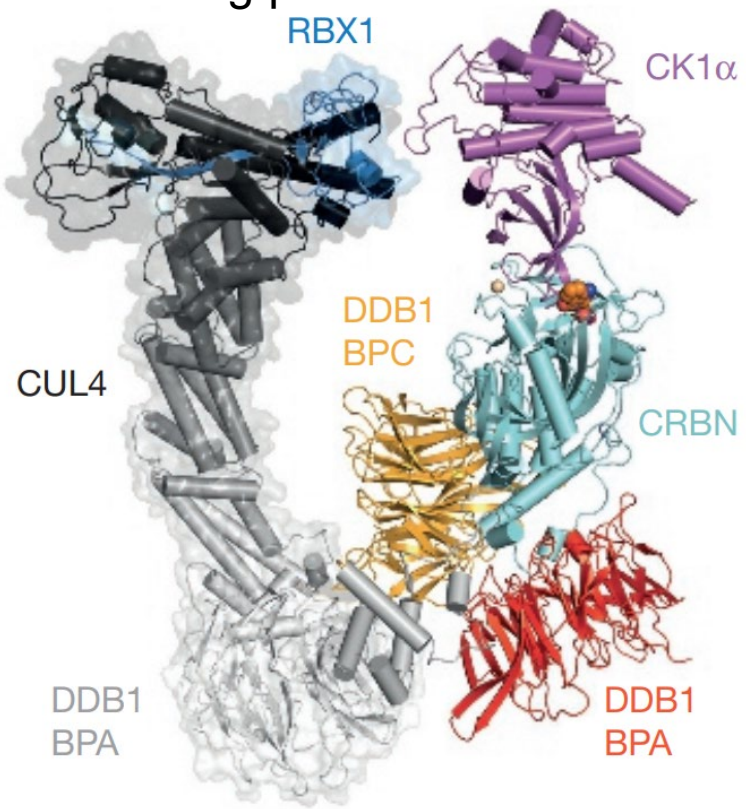

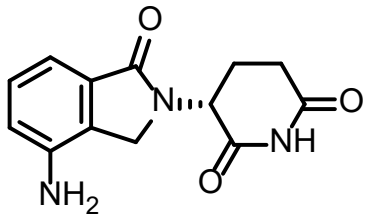

Lenalidomide

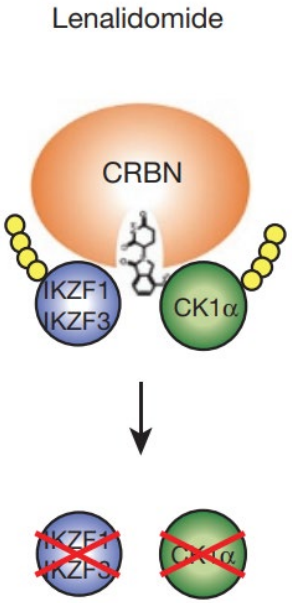

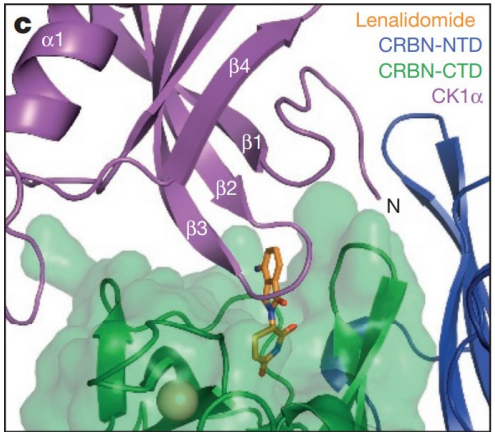

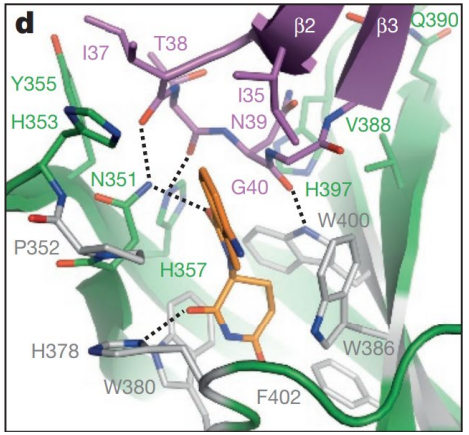

Krönke, J., Fink, E., Hollenbach, P. et al. *Nature,* **2015**, *523*, 183.
Petzold, G., Fischer, E., Thomä, N. *Nature,* **2016,** *532*, 127.

Discovery of neosubstrates

- In 2016, G1 to S phase transition 1 (GSPT1) was identified as a CC-885-dependent neosubstrate. its deletion causes G1 arrest.

- The isoindolinone is close to the β-hairpin loop of GSPT1 and the urea groups of CC-885 also contribute to its interaction with CRBN and GSPT1.

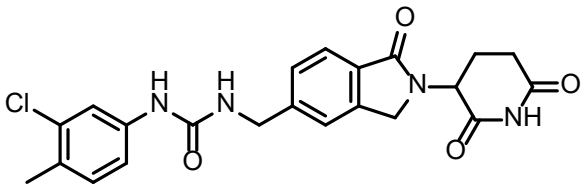

CC-885

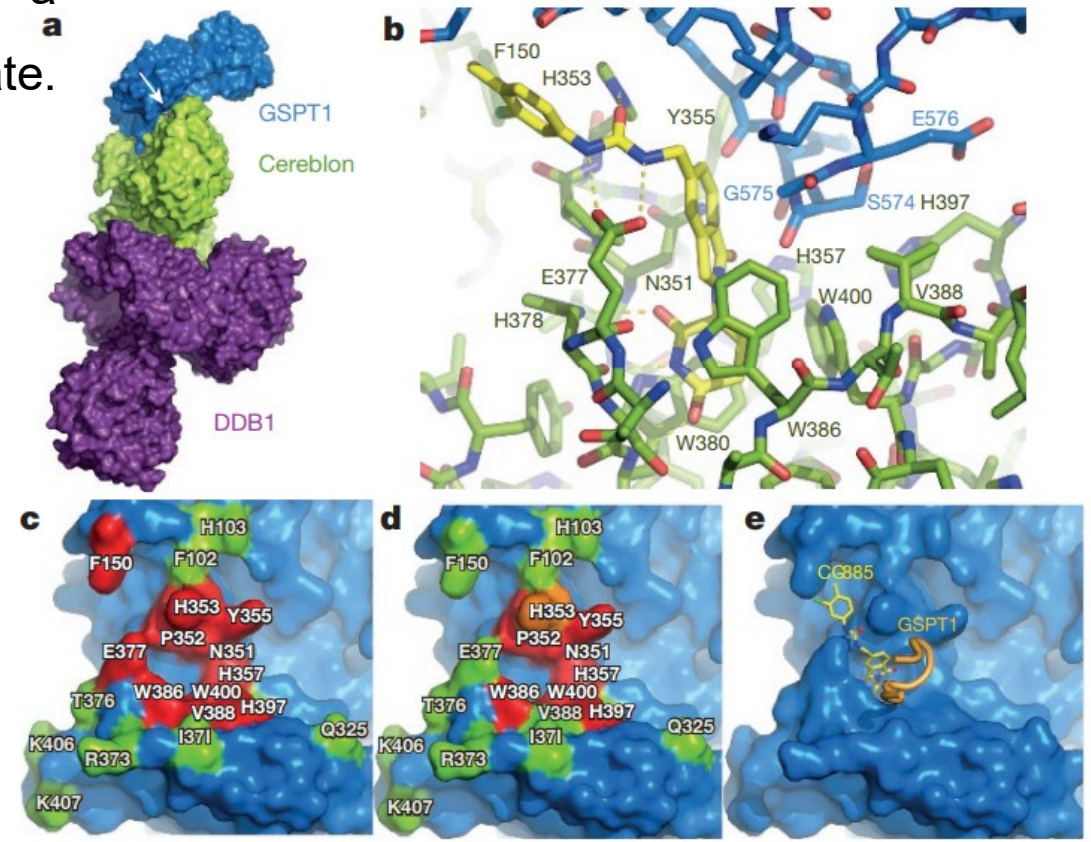

Matyskiela, M., Lu, G., Ito, T. et al. *Nature,* **2016**, *535*, 252.

Discovery of neosubstrates

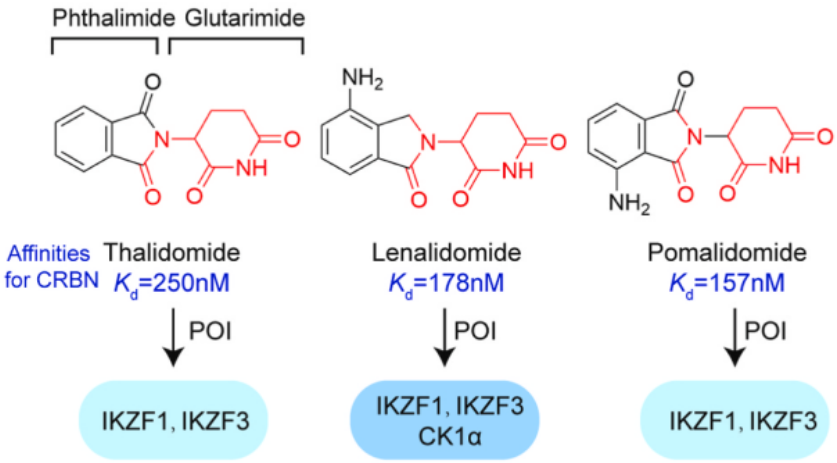

- Dozens of transcription factors or other proteins can be degraded
- Similar binding mechanism through appropriate modification of the isoindolinone fragment

Molecular glues for CRL4^{CRBN}			
Thalidomide	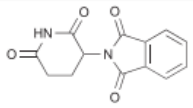	IKZF1, IKZF3, ZNF692, ZNF276, SALL4, RNF166, ZBTB16, FAM83F, p63	(Asatsuma-Okumura et al., 2019; Donovan et al., 2018; Sievers et al., 2018; Yamanaka et al., 2020)
Lenalidomide	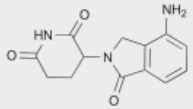	IKZF1, IKZF3, ZFP91, ZFP692, ZNF276, ZNF653, ZNF827, SALL4, RNF166, WIZ1, CK1α, FAM83F, RAB28	(Donovan et al., 2018; Krönke et al., 2014, 2015; Lu et al., 2014; Sievers et al., 2018; Yu et al., 2019)
Pomalidomide	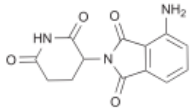	IKZF1, IKZF3, ZFP91, ZFP692, ZNF276, ZNF653, ZNF827, SALL4, RNF166, GZF1, ZBTB39, ZNF98, WIZ1, ZBTB16, FAM83F, RAB28, DTWD1	(An et al., 2017; Donovan et al., 2018; Krönke et al., 2014; Lu et al., 2014; Matyskiela et al., 2020b; Sievers et al., 2018; Yu et al., 2019)
Avadomide (CC-122)	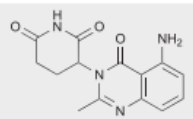	IKZF1, IKZF3, ZFP91	(Hagner et al., 2015)
5-hydroxythalidomide	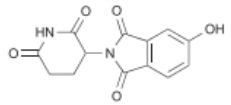	SALL4, ZBTB16	(Furihata et al., 2020; Yamanaka et al., 2020)
FPFT-2216	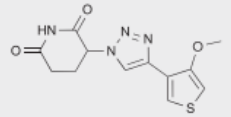	IKZF1, CK1α	(Gemechu et al., 2018)
Iberdomide (CC-220)	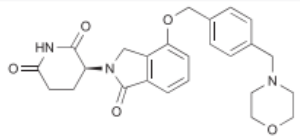	IKZF1, IKZF3, ZFP91, ZNF98	(Donovan et al., 2018; Matyskiela et al., 2018)
CC-647	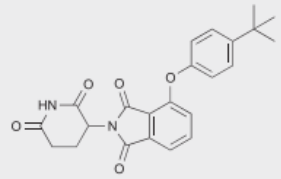	ZBTB16	(Matyskiela et al., 2020b)

Kozicka, Z., Thomä, N. H. *Cell Chem. Biol.* **2021**, *28*, 1032.

Allostery of CRBN when binding

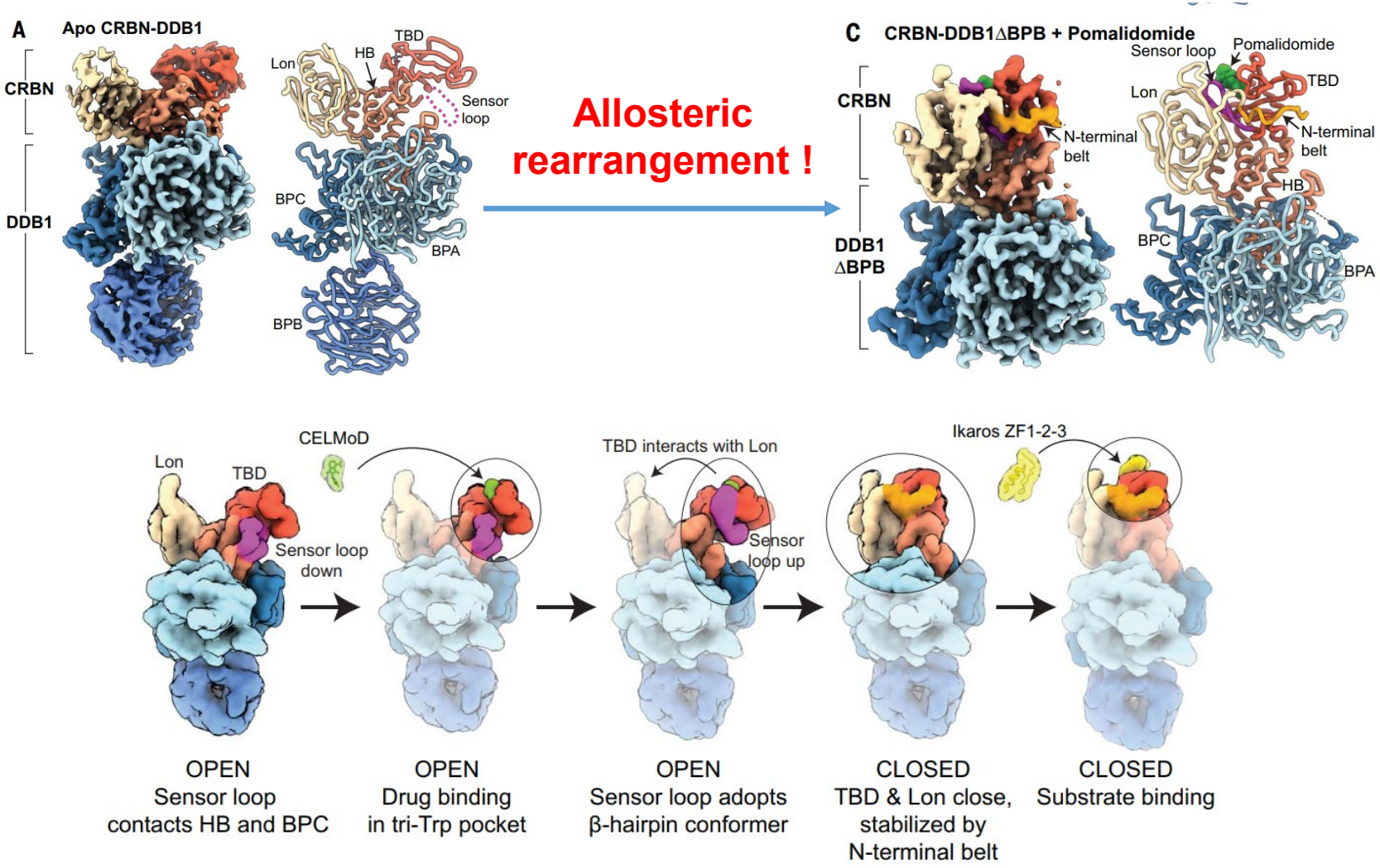

Watson, E. R. et al. *Science,* **2022**, *378*, 549.

Discovery of physiological degrons

- post-translational modifications that arise from intramolecular cyclization of glutamine or asparagine residues, are physiological degrons on substrates for CRBN.

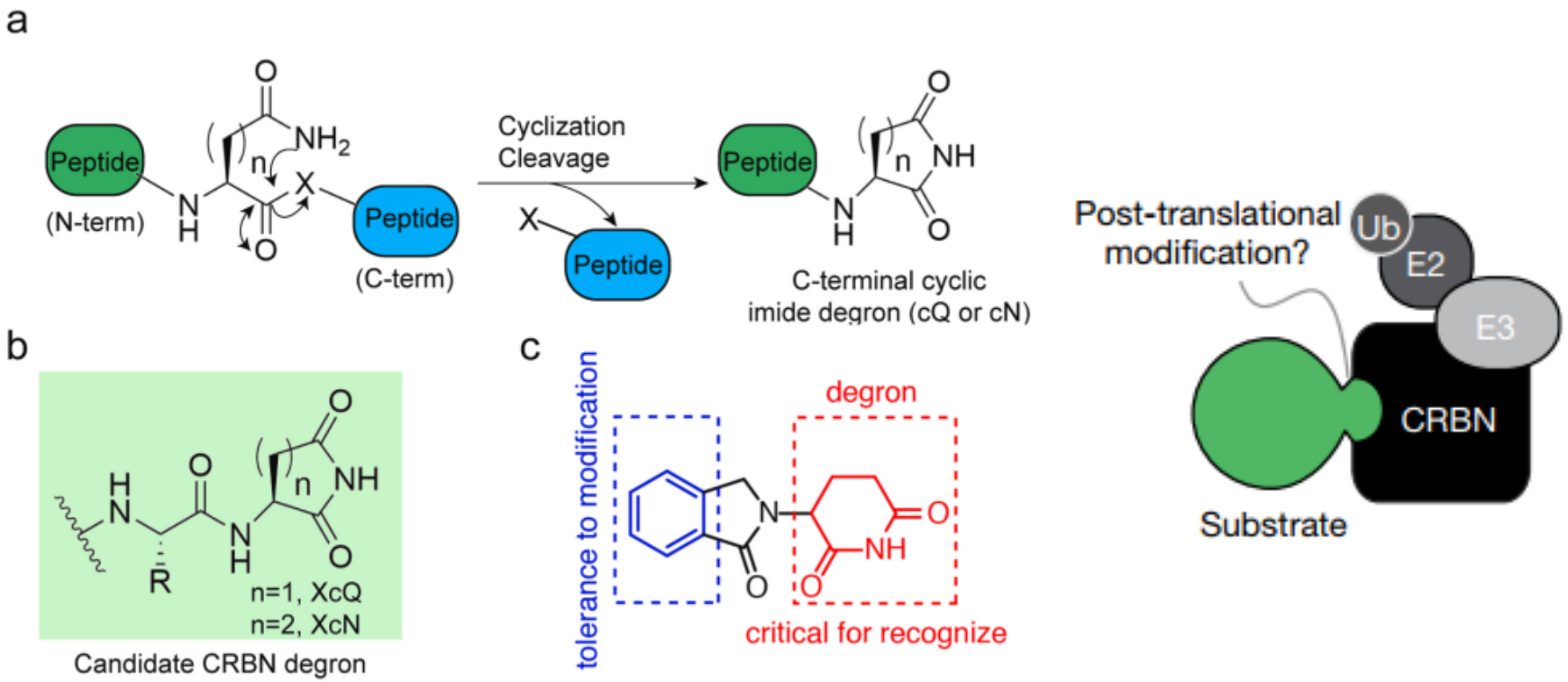

Ichikawa, S., Flaxman, H. A., Xu, W. et al. *Nature*, **2022**, *610*, 775.

History of molecular glue

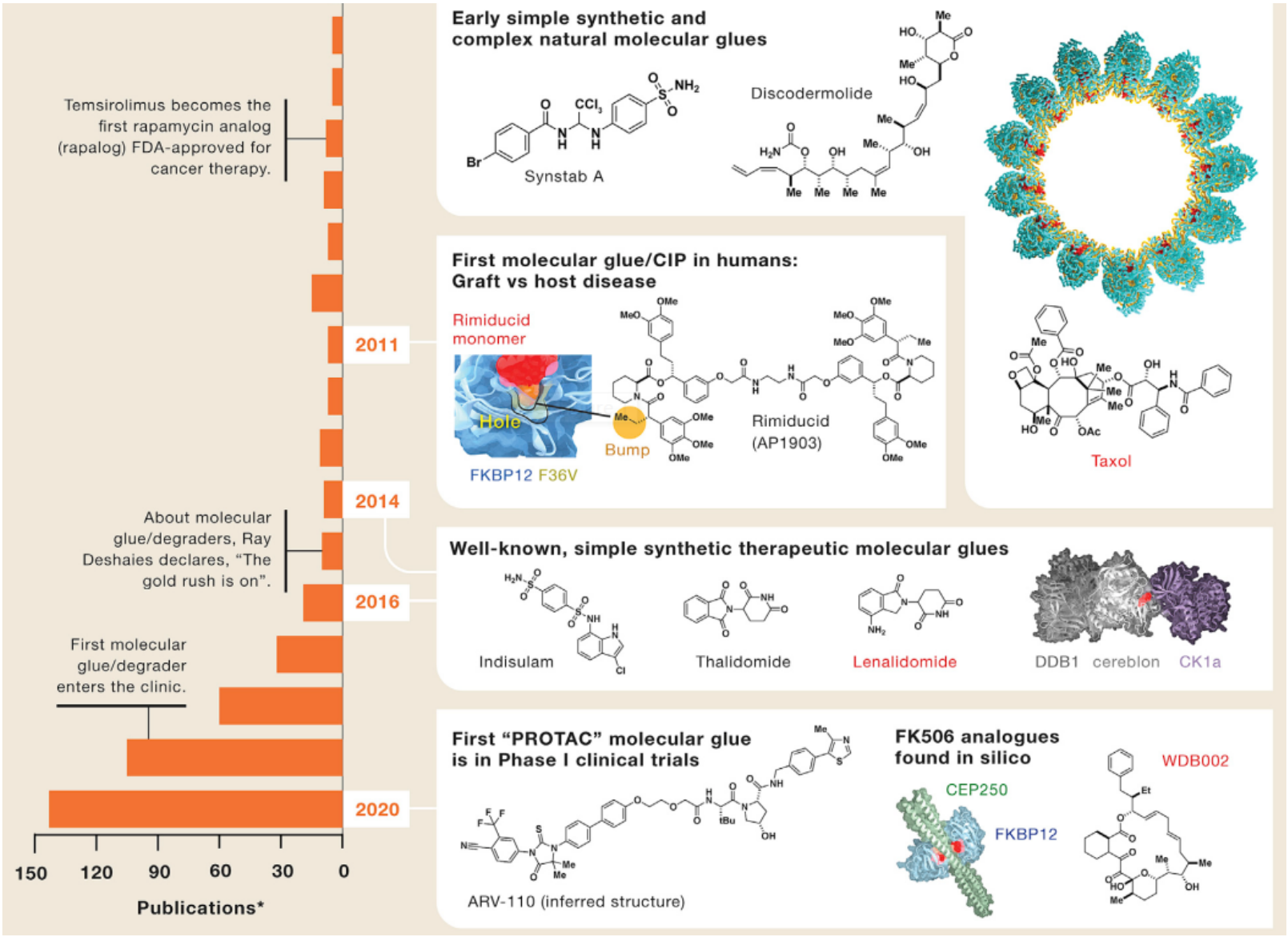

Contents

Anticancer sulfonamides target DCAF15

- Indisulam was found to be specially toxic to a subset of cell lines
- Missense mutations to identify the target protein

indisulam

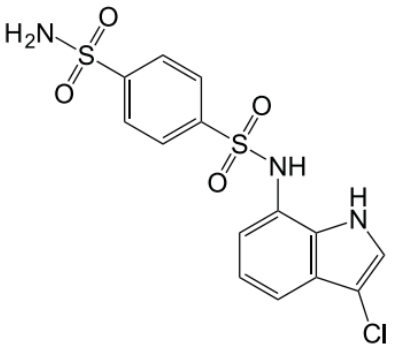

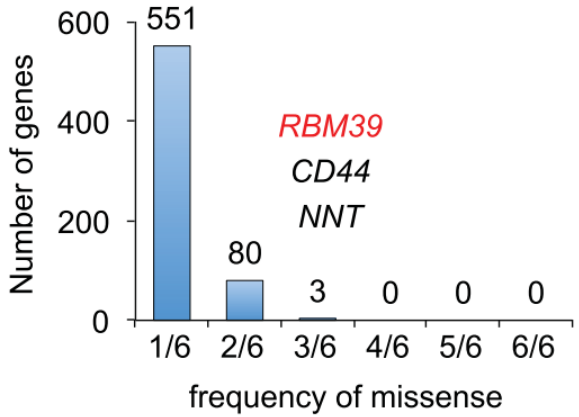

- The amount of RBM39 protein was reduced

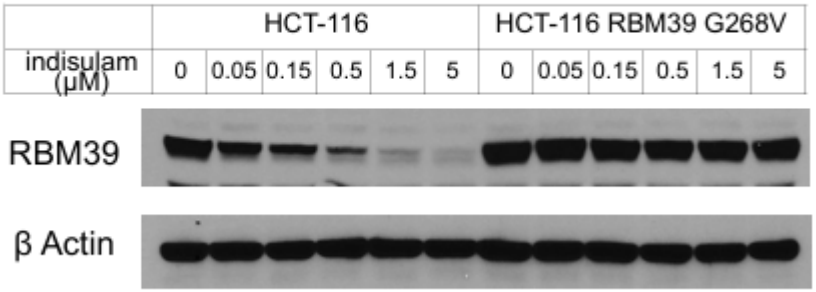

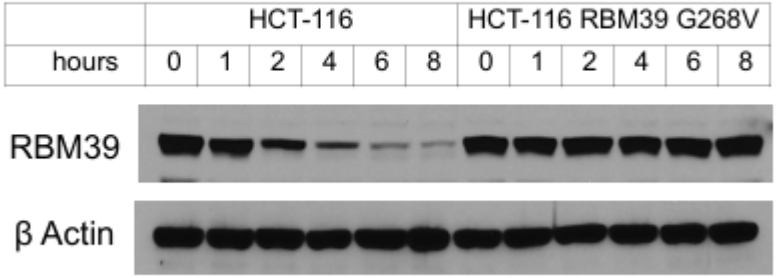

Han, T. et al. *Science,* **2017**, *356*, eaal3755.

Anticancer sulfonamides target DCAF15

F RBM39-3xFLAG IP peptide counts

indisulam	-	+
RBM39	267	259
CUL4A	1	11
CUL4B	0	16
DDB1	5	52
DDA1	0	4
DCAF15	0	11

- CRISPR-Cas9 engineering to introduce a sequence encoding a C-terminal 3×FLAG tag into endogenous RBM39.
- purify RBM39-3×FLAG complexes with anti-FLAG beads from lysate isolated from cells treated with either dimethyl sulfoxide (DMSO) or indisulam.

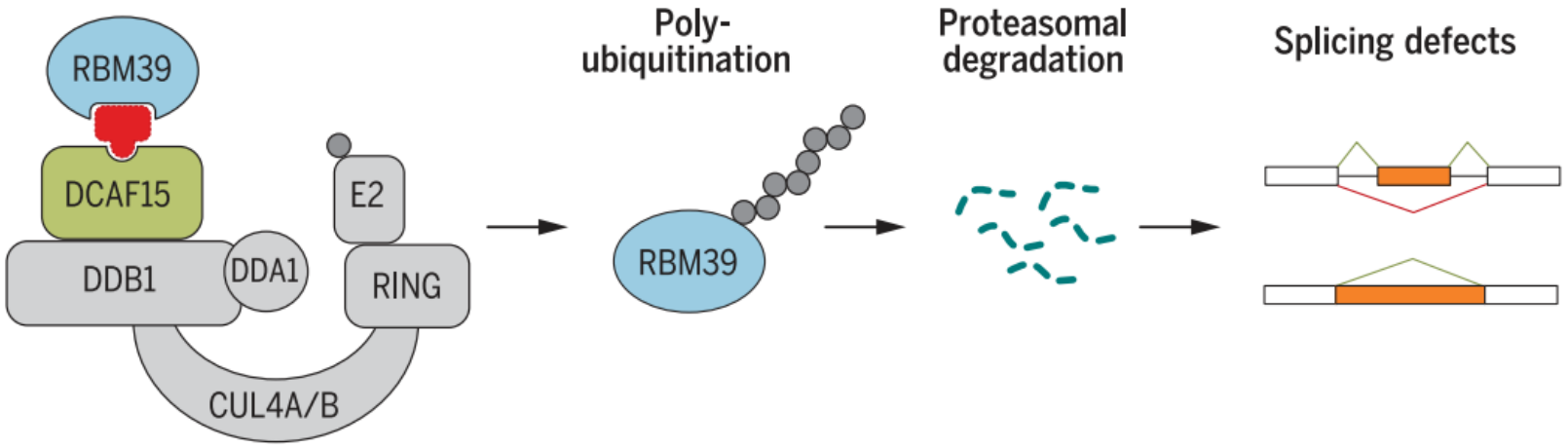

Han, T. et al. *Science,* **2017**, *356*, eaal3755.

Anticancer sulfonamides target DCAF15

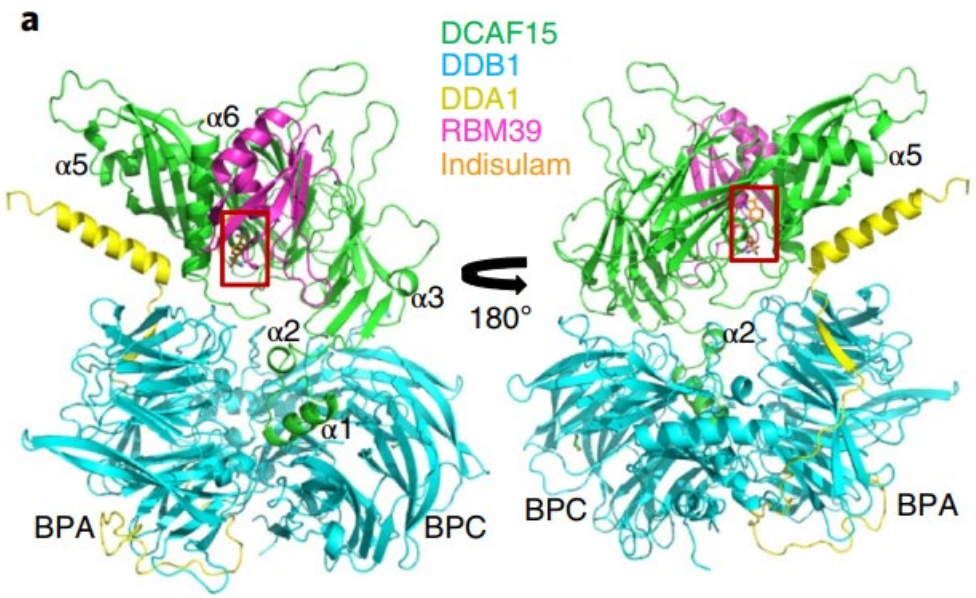

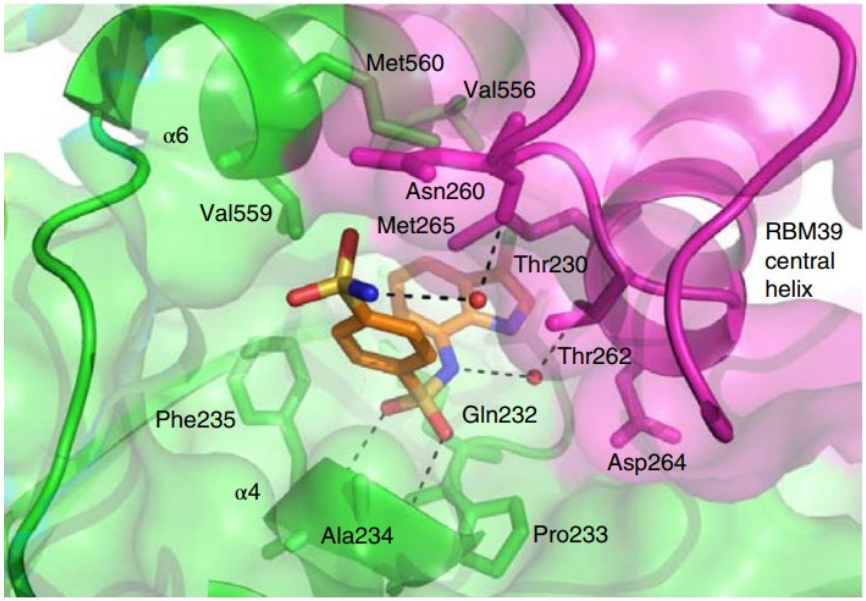

- non-polar surface contacts are key contributors to the RBM39–DCAF15 interaction
- Indisulam coordinates several direct and water-mediated interactions with both RBM39 and DCAF15 and binds the DCAF15 complex with weak affinity (>50μM), but more potently in the presence of RBM39

Bussiere, D. E., Xie, L., Srinivas, H. et al. *Nat. Chem. Biol*. **2020**, *16*, 15.

Other works

Molecular glues for $CRL4^{DCAF15}$			
Indisulam	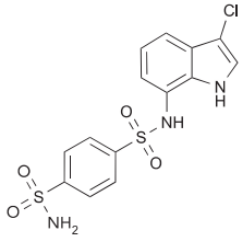	RBM39, RBM23	(Han et al., 2017; Ting et al., 2019; Uehara et al., 2017)
E7820	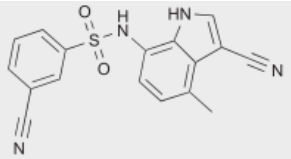	RBM39, RBM23	(Faust et al., 2020; Ting et al., 2019; Uehara et al., 2017)
Tasisulam	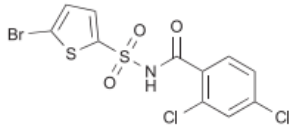	RBM39, RBM23	(Han et al., 2017; Ting et al., 2019)
CQS (chloroquinoxaline sulfonamide)	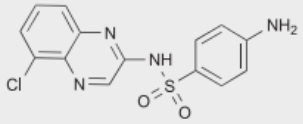	RBM39, RBM23	(Han et al., 2017; Ting et al., 2019; Uehara et al., 2017)
dCeMM1	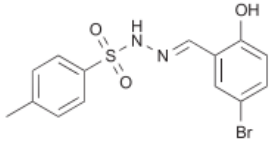	RBM39	(Mayor-Ruiz et al., 2020)

Kozicka, Z., Thomä, N. H. *Cell Chem. Biol.* **2021**, *28*, 1032.

A new mechanism

- Correlate drug-sensitivity data for 4,518 drugs against 578 cancer cell lines with the respective mRNA levels of 499 E3 ligase components.

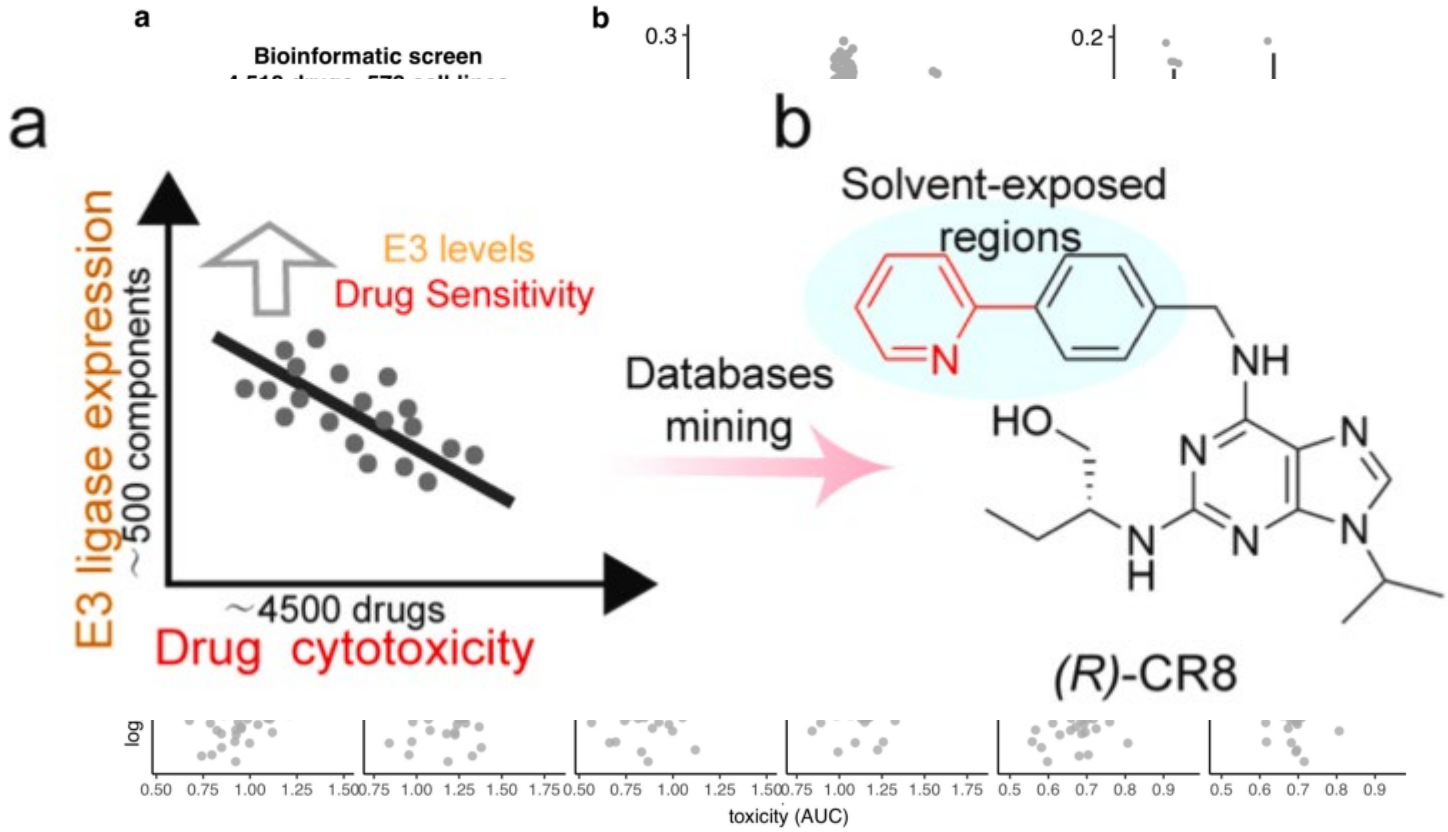

Słabicki, M., Kozicka, Z., Petzold, G. et al. *Nature,* **2020**, *585*, 293.

Discovery of target proteins

- Quantitative proteome-wide mass spectrometry to evaluate protein abundance after treating cells with (R)-CR8.
- Cyclin K was the only protein that consistently showed a decrease in abundance after addition of (R)-CR8

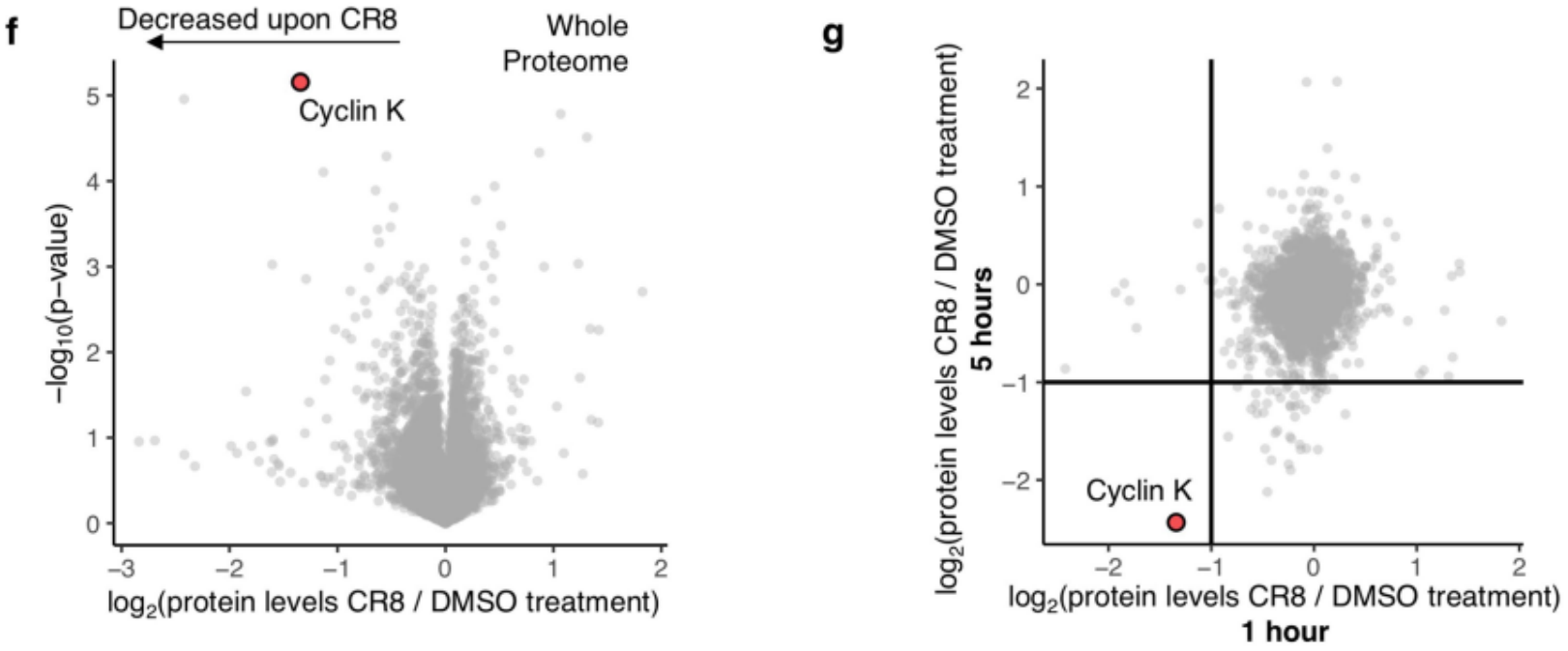

Słabicki, M., Kozicka, Z., Petzold, G. et al. *Nature,* **2020**, *585*, 293.

CR8 directly binds to DDB1

- Other E3 ligase components beyond the E3 substrate receptor may be co-opted to position target proteins.
- This weak interaction is strengthened 500- to 1,000-fold upon treatment with the CDK12 inhibitor CR8.

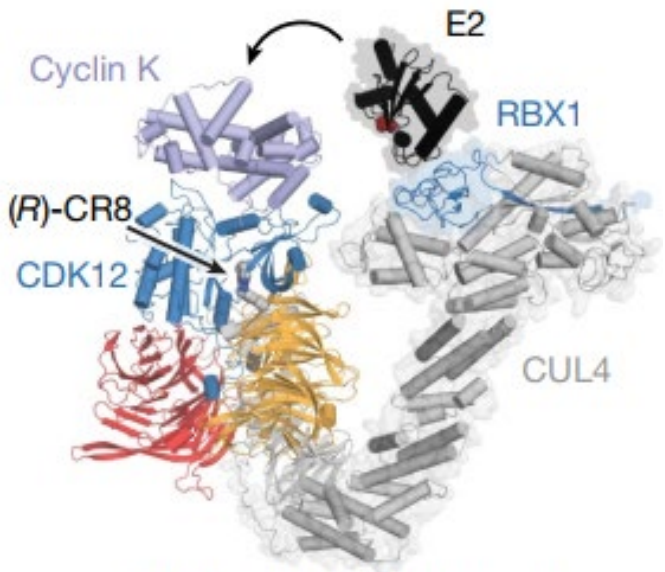

CUL4–RBX1–DDB1 bound to CR8-engaged CDK12–cyclin K

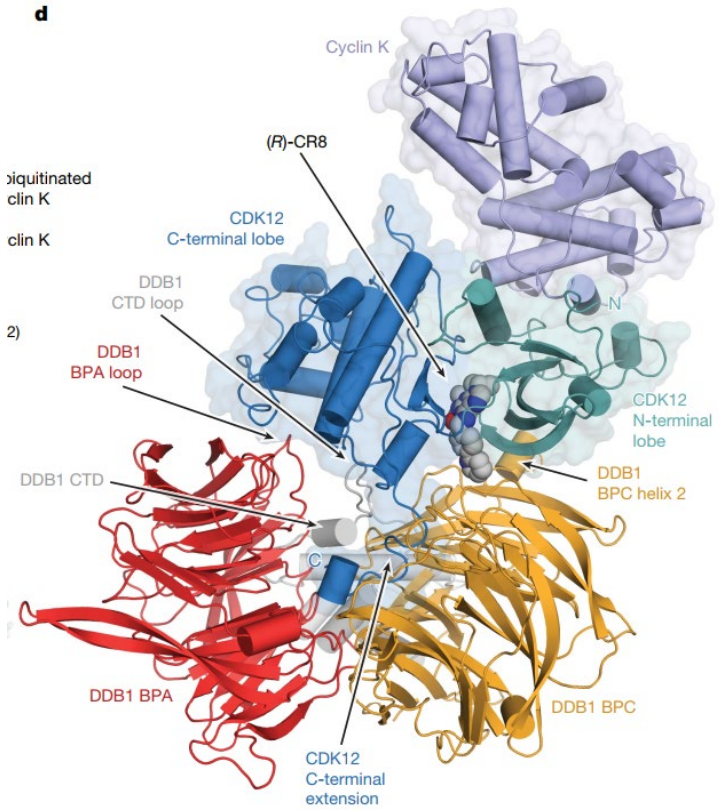

Słabicki, M., Kozicka, Z., Petzold, G. et al. *Nature,* **2020**, *585*, 293.

CR8 directly binds to DDB1

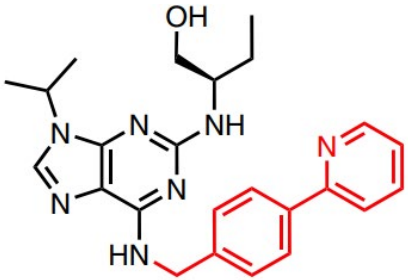

CR8 (**1**)

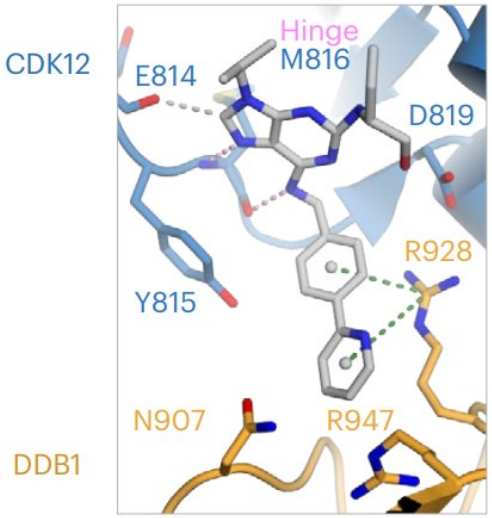

- CR8 bound to the CDK12 kinase active site, and its hydrophobic, surface-exposed phenylpyridine ring acted as a molecular glue, providing interactions with residues in DDB1.

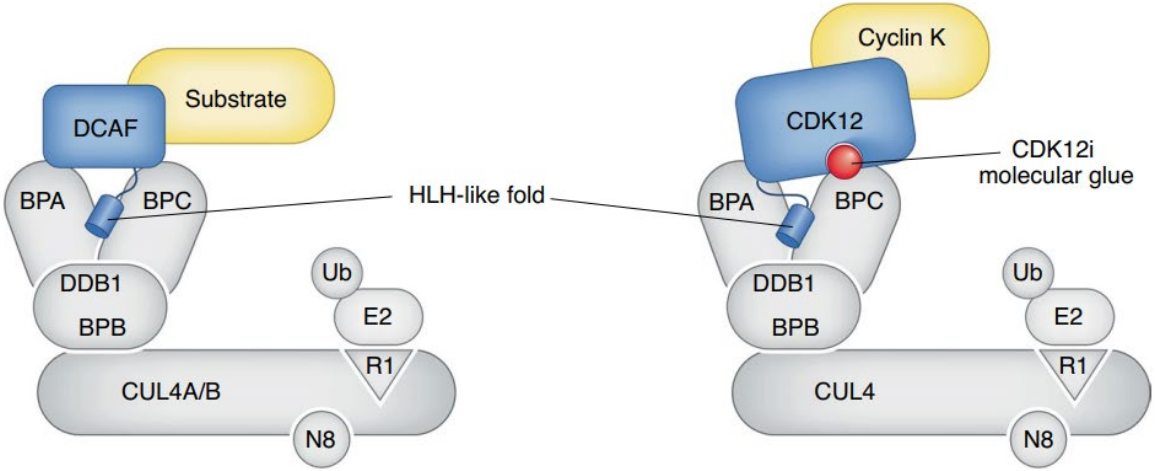

Kozicka, Z., Suchyta, D. J., Focht, V. et al. *Nat. Chem. Biol*. **2024,** *20*, 93.
Besten, W. D., Lipford, J. R. *Nat. Chem. Biol.* **2020**, *16*, 1157.

Other works

CR8	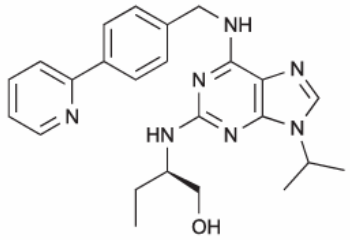	cyclin K	(Słabicki et al., 2020a)
dCeMM2	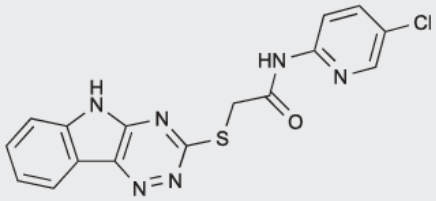	cyclin K	(Mayor-Ruiz et al., 2020)
dCeMM3	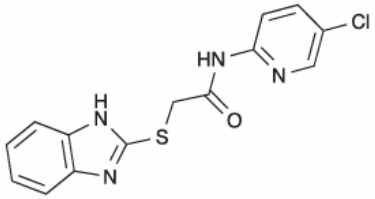	cyclin K	(Mayor-Ruiz et al., 2020)
dCeMM4	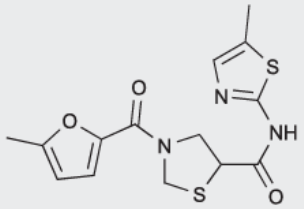	cyclin K	(Mayor-Ruiz et al., 2020)

- Chemical alteration of surface-exposed moieties can confer gain-of-function glue properties to an inhibitor, through which target-binding molecules could be converted into molecular glues.

Kozicka, Z., Thomä, N. H. *Cell Chem. Biol.* **2021**, *28*, 1032.

Contents

Polymerization caused by MGs

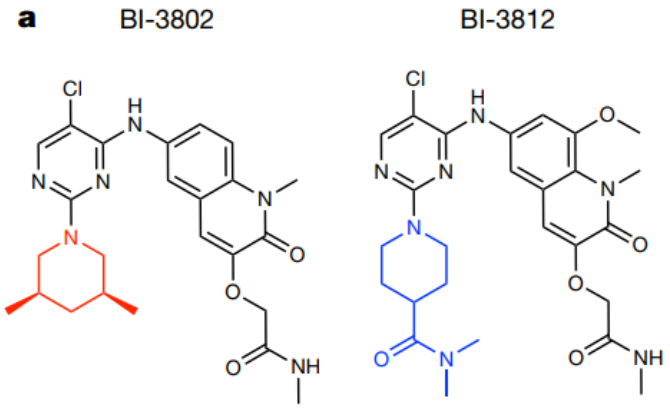

- The glue binds a groove between dimers of the Bric-a-brac (BTB)` domain of BCL6 and promotes polymerization primarily through hydrophobic interactions.
- The ability to “glue” is achieved via solvent exposed, hydrophobic groups.

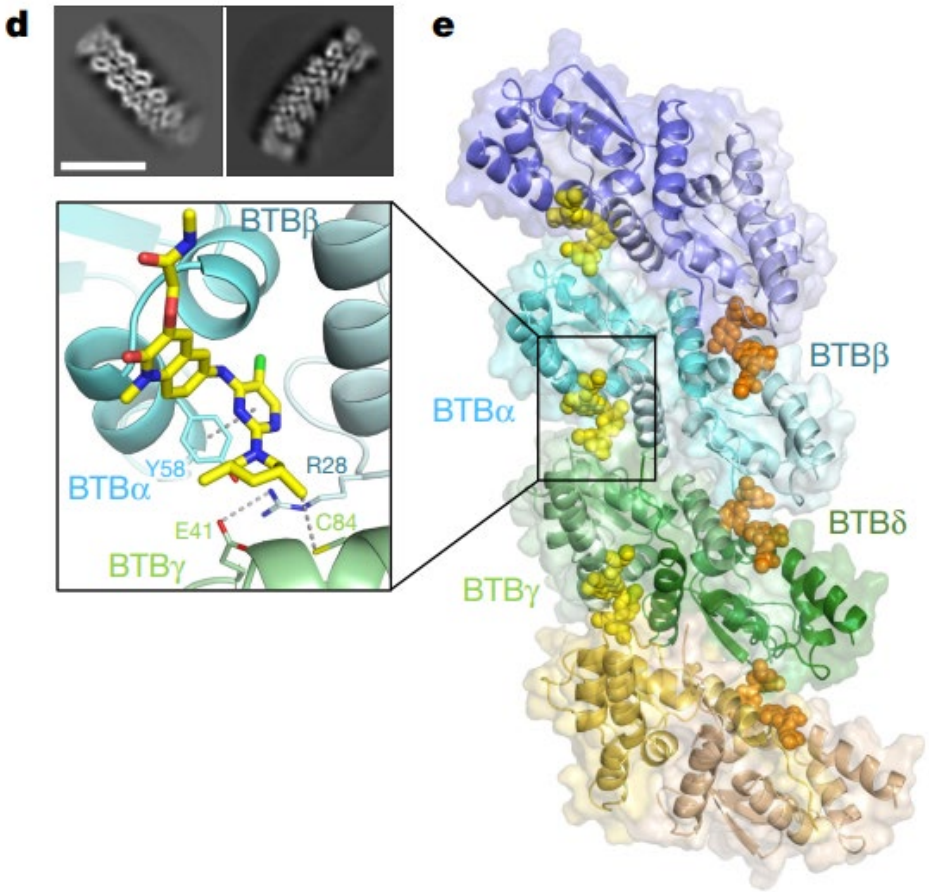

Słabicki, M., Yoon, H., Koeppel, J. et al. *Nature,* **2020**, *588*, 164.

Degradation by autophagosome

- Microarray screening to identify small molecules that selectively induce the interaction of mutant huntingtin protein (mHTT) and LC3
- ATTECs achieve selectivity by engaging a 72 glutamine polyQ region that is absent in the WT allele.

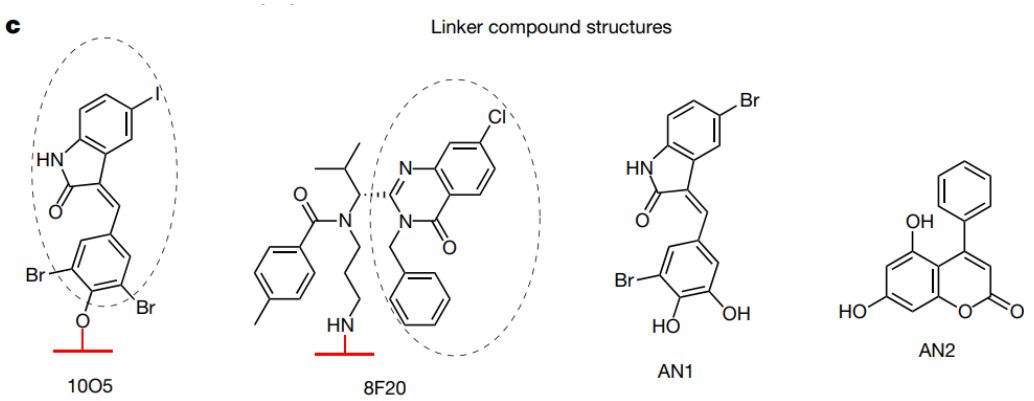

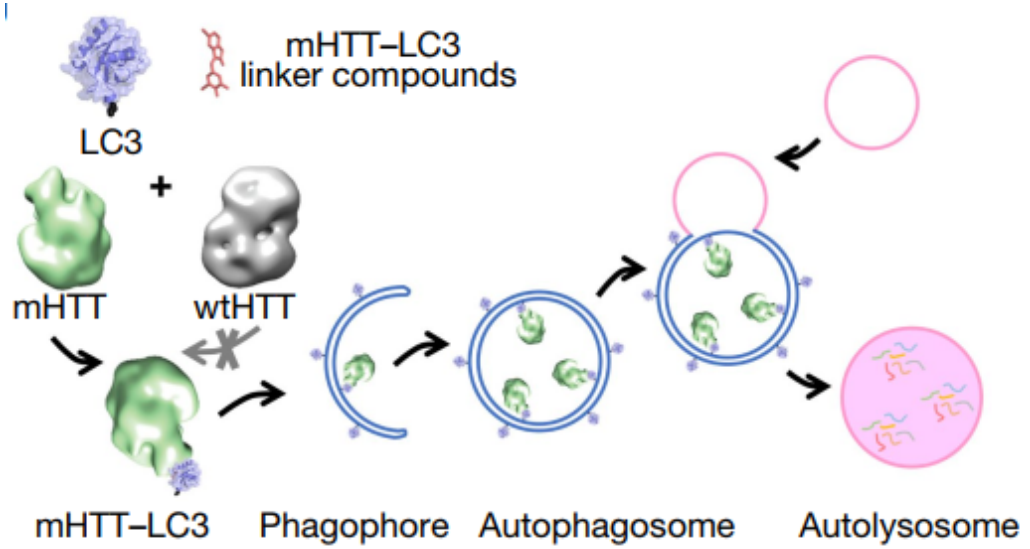

Li, Z., Wang, C., Wang, Z. et al. *Nature,* **2019**, *575*, 203.

Disrupt the PPI between CDK2 and cyclin A

- Cavity analysis and pocket detection in silico
- High throughput screening for candidates

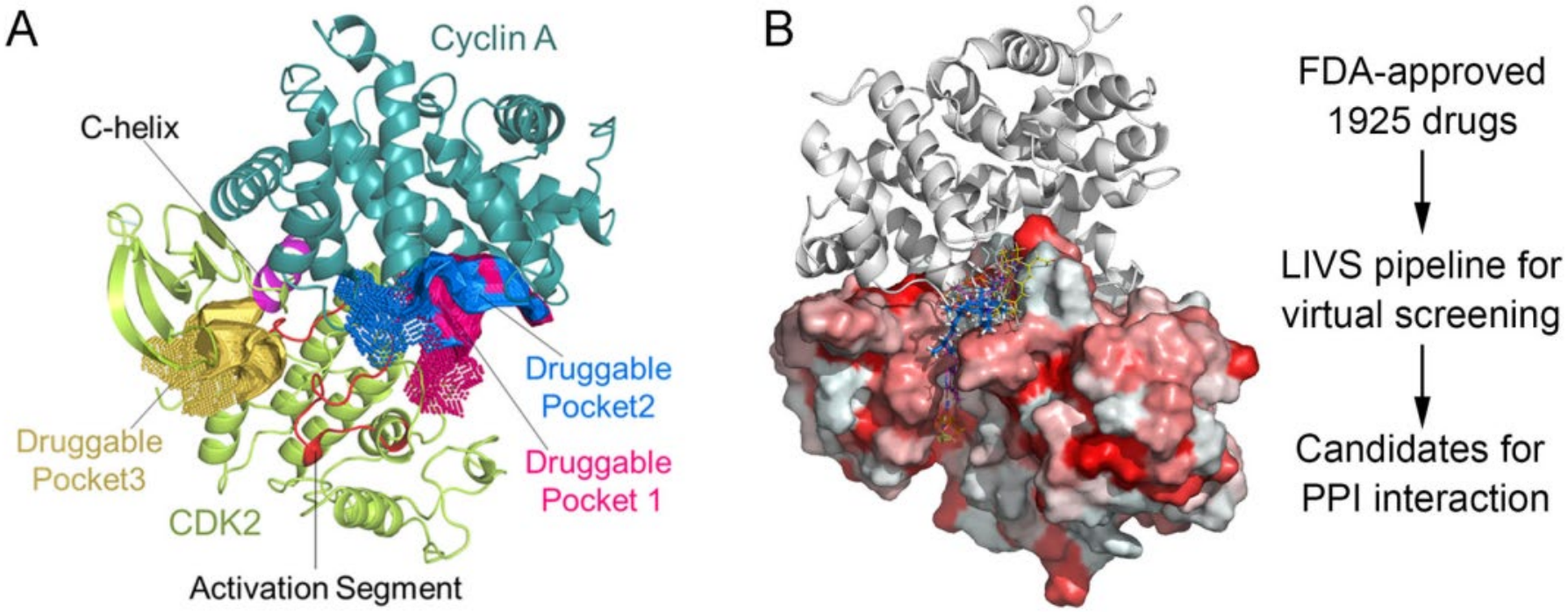

Zhang, J., Gan, Y., Li, H. et al. *Nat. Commun.* **2022**, *13*, 2835.

Disrupt the PPI between CDK2 and cyclin A

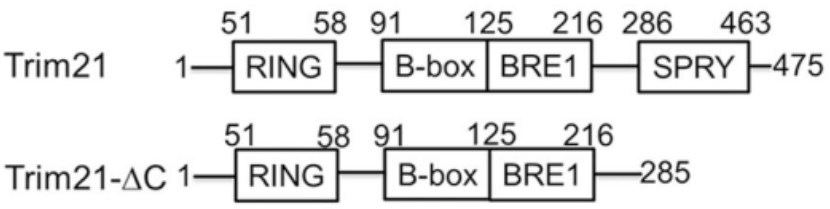

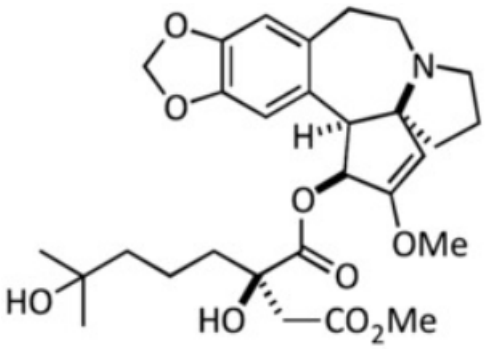

(–)-homoharringtonine (HHT)

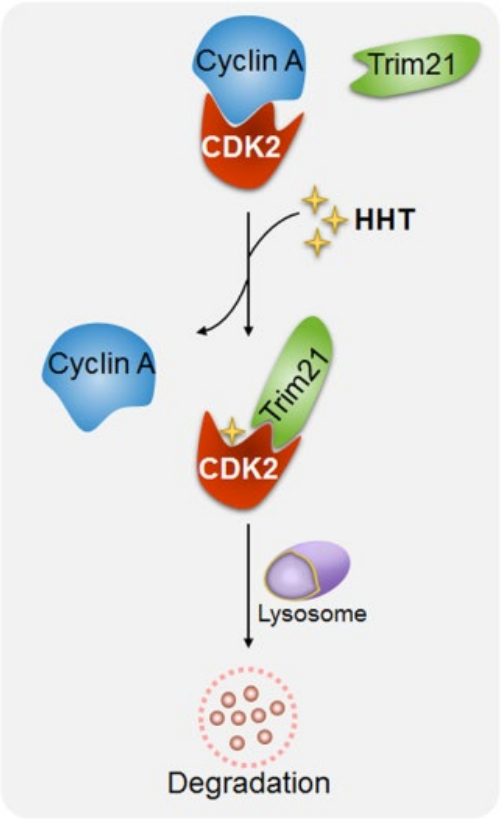

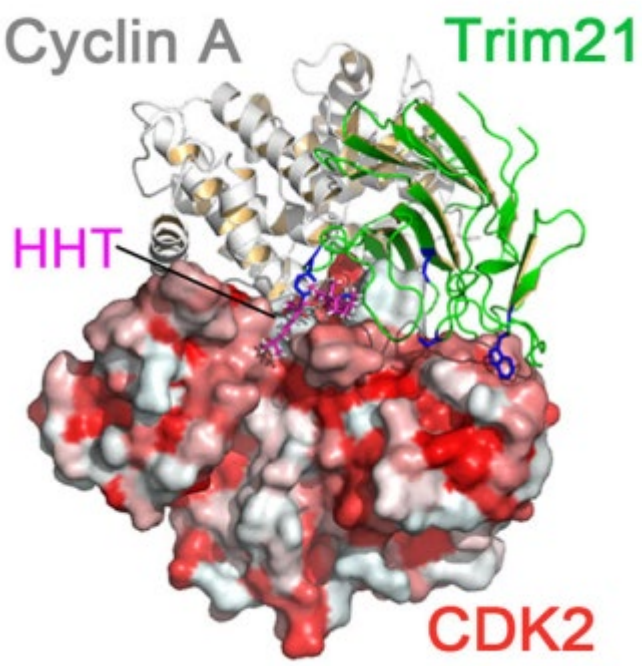

Zhang, J., Gan, Y., Li, H. et al. *Nat. Commun.* **2022**, *13*, 2835.

Contents

Target the active state of mutant KRAS

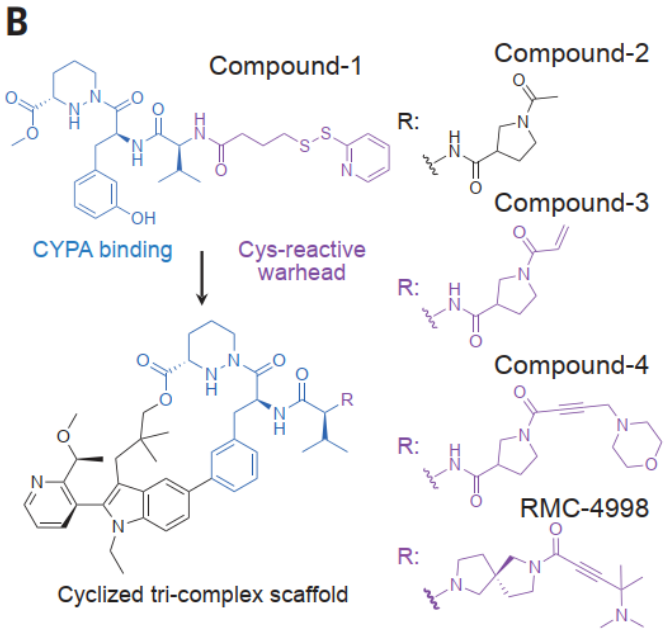

- $KRAS^{G12C}$ is the most frequent KRAS mutation in non–small-cell lung cancer
- RMC-4998 bound to CYPA reversibly to form a low-affinity binary complex (K_d = 1.09 μM) and create a neomorphic interface with affinity for $KRAS^{G12C}$

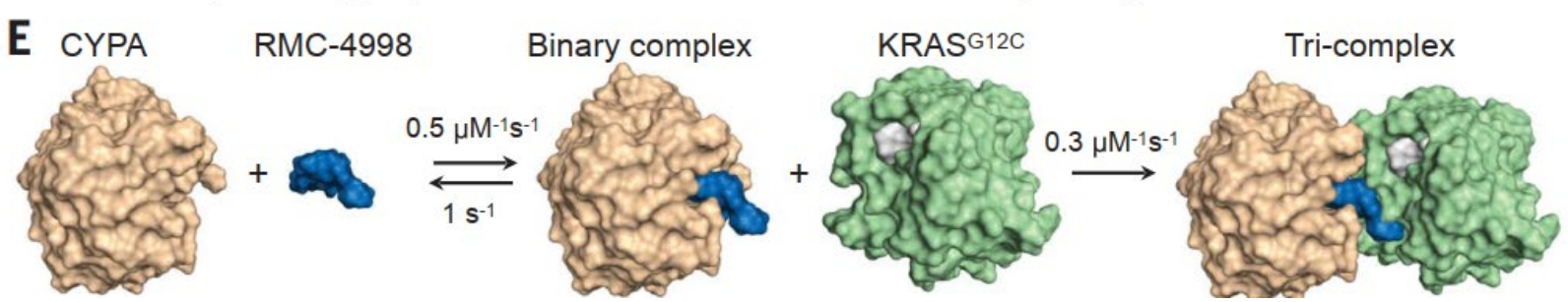

Schulze, C. J. et al. *Science,* **2023**, *381*, 794.

Target the active state of mutant KRAS

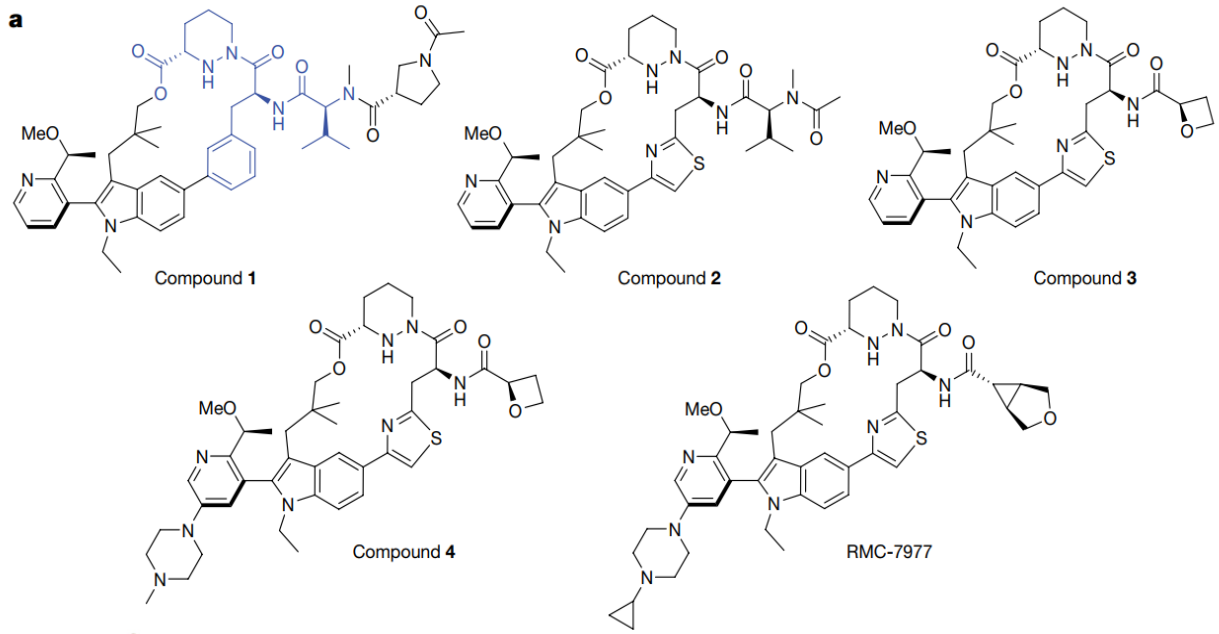

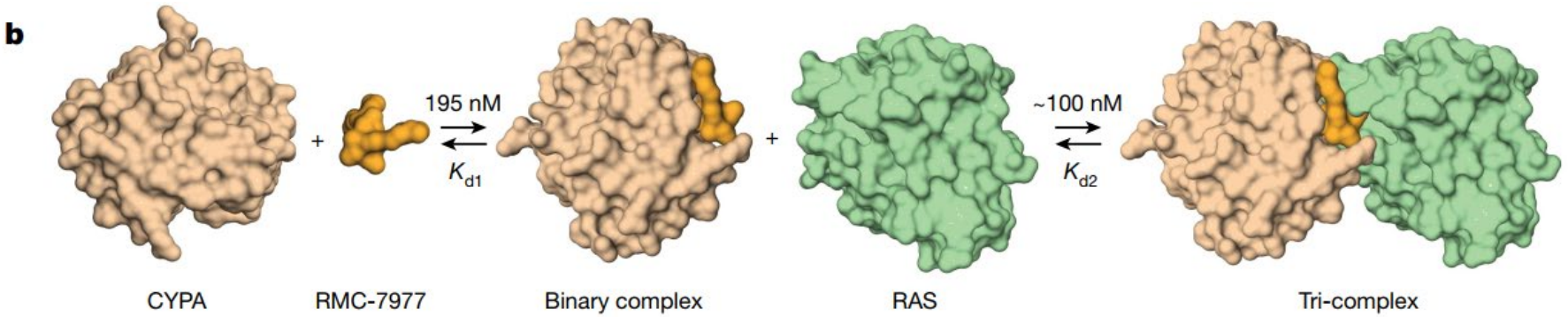

Holderfield, M., Lee, B. J., Jiang, J. et al. *Nature*, **2024**, https://doi.org/10.1038/s41586-024-07205-6.

Rational design of molecular glues

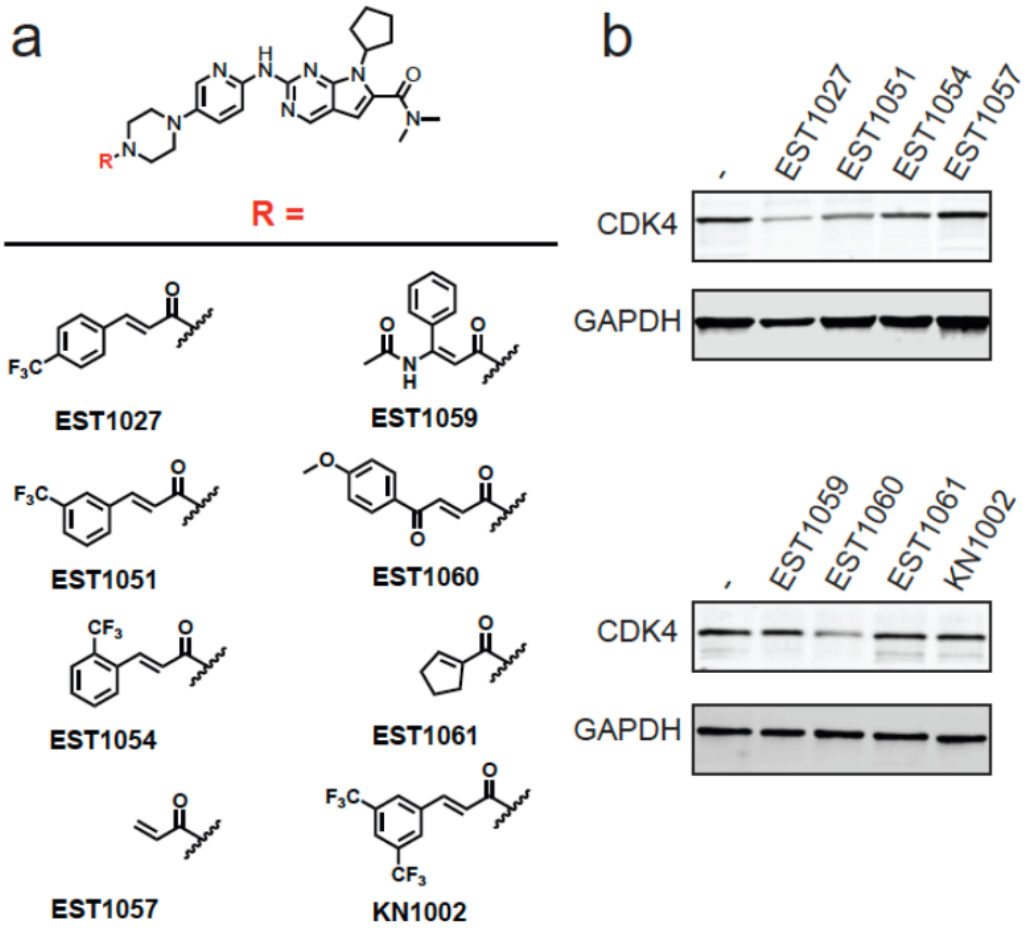

The covalent recognition of E3 ubiquitin ligases RNF126

Toriki, E. S., Papatzimas, J. W., Nomura, D. K. et al. *ACS Cent. Sci.* **2023**, *9,* 915.

Rational design of molecular glues

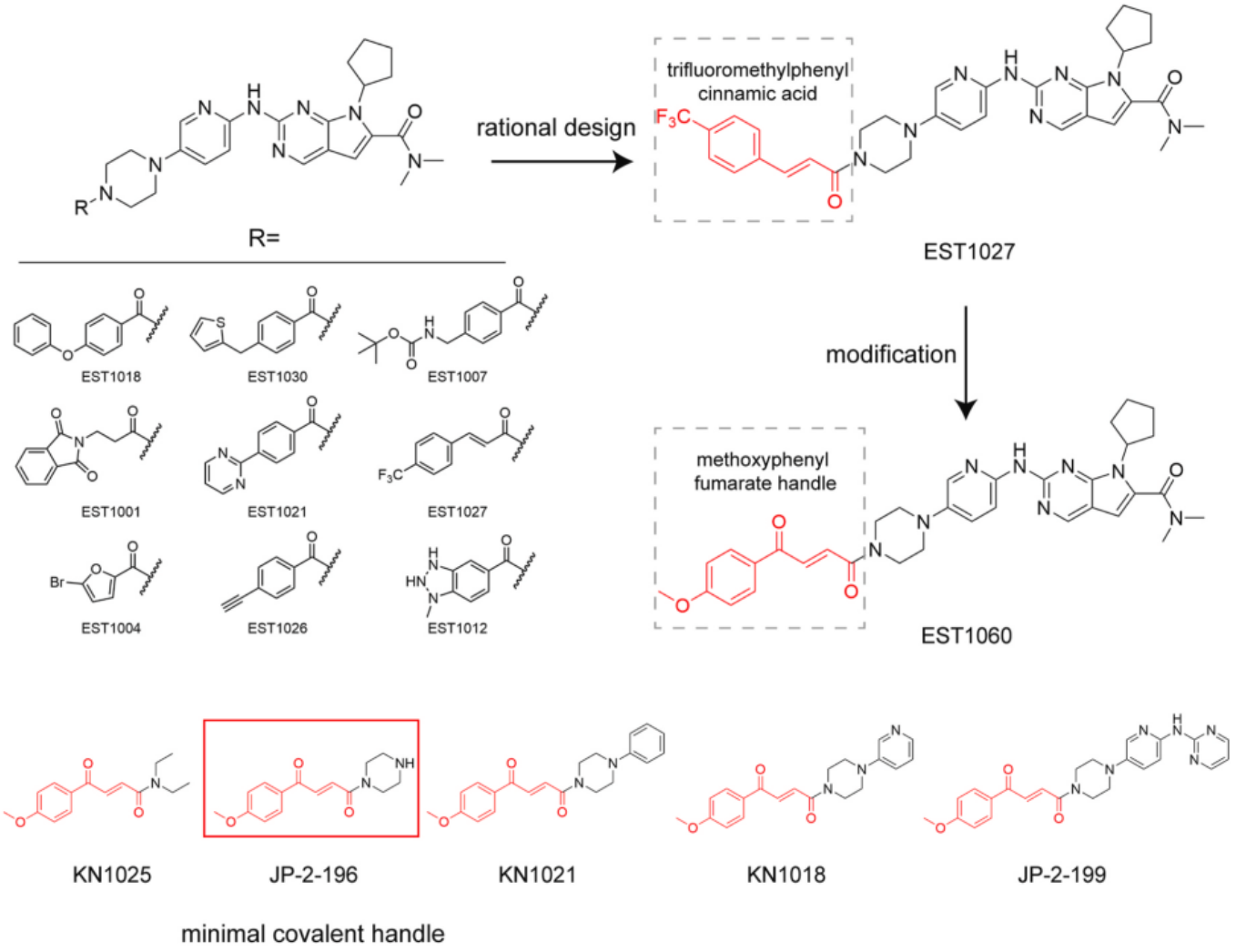

Toriki, E. S., Papatzimas, J. W., Nomura, D. K. et al. *ACS Cent. Sci.* **2023**, *9,* 915.

Summary

Advantages

- Expand the spectrum of druggable target proteins
- Possess a catalytic mechanism of action, which is superior to conventional small molecules with the stoichiometric mode of action

Disadvantages

- E3 ubiquitin ligase and a neosubstrate must exhibit excellent surface complementarity.

Methods

- Screening based on the relationship between E3 ligase activity and drug toxicity
- Screening based on phenotypic-gene relationship

Mechanism of MGs

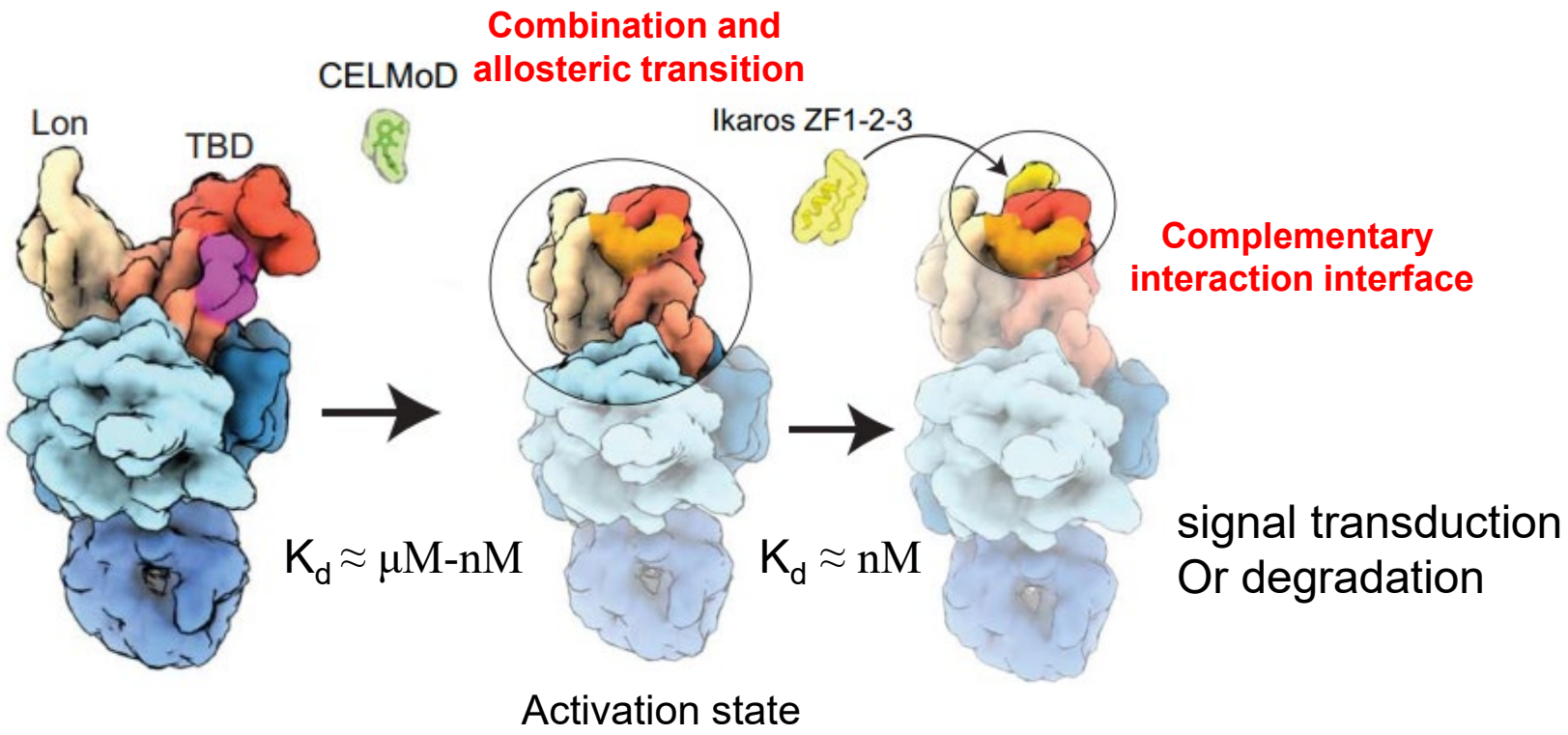

Driving force:

- hydrophobic interaction
- hydrogen bond
- π-π interaction or π-cation interaction

Mostly used functional group:

Aromatic ring

(Located on the surface of protein and exposed to solvent)

Edmond R. Watson et al. *Science* **2022**, *378*, 549-553.

Molecular glue and PROTAC

	molecular glue	PROTAC
mechanism	binds E3 or target protein induces PPI	binds target and E3
target protein	to be determined	predictable
discovery strategy	historically serendipitous discovery	rational design
feature	monovalent	bivalent
linker	without linker	with linker
molecular weight	lower	higher
rule of five	typically within	beyond
binding pocket in the target protein	nonessential	required

PROTACs induce proximity of the target protein to the E3 ligase and do not change protein-protein interactions most of time.